of Bmp2, Bmp7, Fgf4, Fgf7 and Shh, while it unexpectedly increased that of Fgf2 (data not shown). To confirm that Fgf2 expression is regulated by AG17 and PDGF, we examined its expression in SF2 cells. Interestingly, AG17 induced Fgf2 expression, whereas PDGF-AA inhibited that expression in SF2 cells (Fig. 6A). Furthermore, PDGF-AA induced ameloblastin expression, whereas AG17 inhibited it (Fig. 6B). These results show that PDGF signalling functions as a modulator of other potent factors, including Fgf2 and ameloblastin, to control dental epithelium differentiation.

4. Discussion

In the present study, we found that PDGF-BB induces dental mesenchyme proliferation and PDGF-AA accelerates cusp formation. In addition, endogenous PDGFs were shown to be important for tooth germ growth and cusp formation, based on our experiments with AG17 treatment. Furthermore, our results showed that PDGF-AA regulates the expressions of Fgf2 and ameloblastin in dental epithelial cells, indicating its critical role in dental epithelium differentiation.

PDGFα, a gene coding PDGF-A, is expressed in embryos by several different types of progenitor cells that proliferate and migrate in response to PDGF. For example, PDGFα is expressed in precursor cells that become cranial neural crest cells and is thought to be required for migration of those cells into the brachial arches. PDGFα is also expressed by smooth muscle progenitors in developing lungs and widely throughout the embryonic mesenchyme, while PDGFα-deficient mice have a variety of defects in crest-derived tissues, including gross craniofacial, skeletal and cardiac abnormalities. During tooth development, PDGF-A is highly expressed in dental epithelium and weakly in dental mesenchyme (Fig. 1). PDGF-A and PDGF-B form homodimers, PDGF-AA and PDGF–BB, and a heterodimer, PDGF-AB. The only known receptor for PDGF-AA is PDGFRα, which is expressed in dental mesenchyme and inner enamel epithelium, indicating that PDGF-AA may have effects on inner enamel epithelium and neural crest-derived dental mesenchyme.

Dental cusp malformation in PDGFRα null mutants leads to a critical growth defect and shows the requirement for PDGF signalling in the determination of tooth morphology. Loss of the *Pdgfrα* gene does not have effects on proper odontoblast proliferation and differentiation in the cranial neural crest-derived odontogenic mesenchyme. However, such a lack perturbs formation of the extracellular matrix and organisation of odontoblast cells in the cusp forming area, resulting in a dental cusp growth defect.[13] PDGF-AA and PDGF-BB are able to bind to PDGFRα. In the present experiments, PDGF-BB, but not PDGF-AA, was shown to accelerate dental mesenchymal proliferation. Together, our results suggest that PDGF-BB and PDGFRβ signalling, but not PDGFRα, may be important for dental mesenchymal proliferation.

A previous study used embryonic day 10 mandibular explants cultured in serum-free media and reported that exogenous PDGF-AA enhances tooth development to reach the cap stage with increased tooth size.[17] However, in our experiments with embryonic day 13 tooth germ cultures with a low concentration of serum, we found that treatment with exogenous PDGFs did not have an effect on tooth germ growth (data not shown), in contrast to treatment with AG17. Based on these results together with those showing a high expression of PDGF-A in tooth germs, we propose that the PDGF-AA isoform and its tyrosine kinase receptor, PDGFRα, regulate tooth size and tooth development during odontogenesis via an autocrine mechanism.

We found that PDGF-A was expressed in submandibular gland epithelium, whereas PDGF-B, PDGFRα and PDGFRβ were expressed in mesenchyme. Exogenous PDGF-AA and -BB in submandibular gland organ cultures demonstrated increased levels of branching and epithelial proliferation, though their receptors were found to be expressed in mesenchyme. PDGF-AA and PDGF-BB induced the expression of Fgf7 and Fgf10, indicating that PDGFs regulate Fgf gene expression in submandibular gland mesenchyme. Also, the PDGF receptor inhibitor AG17 inhibited PDGF-induced branching morphogenesis, whereas exogenous Fgf7 and Fgf10 expressions were fully recovered. Together, these results indicate that fibroblast growth factors function downstream of PDGF signalling, and regulate Fgf expression in neural crest-derived mesenchymal cells and submandibular gland branching morphogenesis.[12] Thus, PDGF signalling is a possible mechanism involved in the interaction between epithelial and neural crest-derived mesenchyme. In tooth germ development, we speculate that an important mechanism of tooth morphogenesis via epithelial and mesenchymal interactions functions in submandibular gland morphogenesis, because of similar patterns of expression of PDGFs and their receptors in both submandibular gland and tooth germ cultures. In fact, AG17 partially decreased the expressions of Bmp2, Bmp7, Fgf4, Fgf7 and Shh, and increased that of Fgf2 in tooth germ organ cultures (data not shown). Previous studies have provided critical information regarding the functional significance of the epithelially derived enamel knot in dental cusp formation. The primary enamel knot in the cap stage tooth germ is a transient structure and serves as a signal centre for regulating cusp formation. Multiple growth factors (such as Shh, Bmps, Fgfs and Wnts), transcription factors (such as Msx2 and Lef1) and cell cycle regulators (such as p21) have important functions in regulating dental cusp formation and the fate of epithelial cells in the enamel knot.[1] A decrease in the expressions of Bmps and Shh may be associated with inhibition of cusp formation in the presence of AG17.

Organisation and remodelling of the basement membrane are also important for determination of tooth size and shape. Laminin α5, a basement membrane component, is highly expressed during tooth germ development. Laminin α5 null-mice have small teeth and inhibited cusp formation, because of decreased expressions of Fgf4 and Shh in the enamel knot.[14] Previous studies have shown a dramatic reduction in MMP-2 in neural crest-derived dental mesenchyme and inhibition of cusp formation in PDGFRα null mutants, which suggest a critical role for that extracellular proteinase in normal tooth development.[13,18] The biological function of MMP-2 is critical for breakdown of the basement membrane prior to the formation of dentin and enamel matrix, as well as for extracellular matrix remodelling, as odontoblast cells retreat towards the central part of dental mesenchyme during dental cusp development.[13] These results indicate that a proper

basement membrane is necessary for cusp formation and PDGF signalling may regulate these related processes.

In our experiments, exogenous PDGF-AA reduced Fgf2 expression in the dental epithelial cell line SF2. Previously, Fgf2 was found to potently induce both proliferation and expression of DSPP in immature pulp cells.[19] Furthermore, exogenous Fgf2 decreased the gene expressions of differentiation markers, such as amelogenin, DSPP and alkaline phosphatase, in molars at the bell stage, while abrogation of endogenous Fgf2 by antisense oligonucleotide increased the gene expressions of those differentiation makers, and also significantly enhanced enamel and dentin formation.[20] These findings suggest that Fgf2 at the bell stage regulates cell differentiation and matrix secretion. In addition, the effects of Fgf2 on tooth cells may be regulated by PDGF-AA, while exogenous PDGF-AA induces ameloblastin expression in dental epithelium. Ameloblastin plays an important role in maintaining the differentiation state of ameloblasts, and also serves as a cell adhesion molecule and regulates ameloblast differentiation.[21] That study also showed that a deficiency of ameloblastin causes severe enamel hypoplasia, accelerates the proliferation of dental epithelium and decreases the expression of amelogenin. Administration of exogenous PDGF-AA to dental epithelial cells may be useful for induction of ameloblastin and differentiation of dental epithelium to ameloblasts.

In conclusion, PDGF-A, PDGF-B, PDGFRα and PDGFRβ were found to be expressed during tooth development. AG17 inhibited tooth germ growth and cusp formation, while exogenous PDGF-BB accelerated the proliferation of dental mesenchymal cells and PDGF-AA induced cusp formation. Furthermore, PDGF-AA reduced the expression of Fgf2 and induced ameloblastin expression. Together, our results indicate that PDGFs and their receptors are necessary for tooth development.

Funding

This work was supported in part by grants-in-aid for Research Fellows of the Japan Society for the Promotion of Science from the Ministry of Education, Science and Culture of Japan (17689058 and 20679006 to S. Fukumoto).

Conflicts of interest

None declared.

Ethical approval

Not required.

REFERENCES

1. Jernvall J, Thesleff I. Reiterative signaling and patterning during mammalian tooth morphogenesis. *Mech Dev* 2000;**92**(March (1)):19–29.
2. Andrae J, Gallini R, Betsholtz C. Role of platelet-derived growth factors in physiology and medicine. *Genes Dev* 2008;**22**(May (10)):1276–312.
3. Betsholtz C, Karlsson L, Lindahl P. Developmental roles of platelet-derived growth factors. *Bioessays* 2001;**23**(June (6)):494–507.
4. Hoch RV, Soriano P. Roles of PDGF in animal development. *Development* 2003;**130**(October (20)):4769–84.
5. Bostrom H, Willetts K, Pekny M, Leveen P, Lindahl P, Hedstrand H, et al. PDGF-A signaling is a critical event in lung alveolar myofibroblast development and alveogenesis. *Cell* 1996;**85**(June (6)):863–73.
6. Soriano P. The PDGF alpha receptor is required for neural crest cell development and for normal patterning of the somites. *Development* 1997;**124**(July (14)):2691–700.
7. Sun T, Jayatilake D, Afink GB, Ataliotis P, Nister M, Richardson WD, et al. A human YAC transgene rescues craniofacial and neural tube development in PDGFRalpha knockout mice and uncovers a role for PDGFRalpha in prenatal lung growth. *Development* 2000;**127**(November (21)):4519–29.
8. Leveen P, Pekny M, Gebre-Medhin S, Swolin B, Larsson E, Betsholtz C. Mice deficient for PDGF B show renal, cardiovascular, and hematological abnormalities. *Genes Dev* 1994;**8**(August (16)):1875–87.
9. Soriano P. Abnormal kidney development and hematological disorders in PDGF beta-receptor mutant mice. *Genes Dev* 1994;**8**(August (16)):1888–96.
10. Lindahl P, Johansson BR, Leveen P, Betsholtz C. Pericyte loss and microaneurysm formation in PDGF-B-deficient mice. *Science* 1997;**277**(July (5323)):242–5.
11. Hellstrom M, Kalen M, Lindahl P, Abramsson A, Betsholtz C. Role of PDGF-B and PDGFR-beta in recruitment of vascular smooth muscle cells and pericytes during embryonic blood vessel formation in the mouse. *Development* 1999;**126**(June (14)):3047–55.
12. Yamamoto S, Fukumoto E, Yoshizaki K, Iwamoto T, Yamada A, Tanaka K, et al. Platelet-derived growth factor receptor regulates salivary gland morphogenesis via fibroblast growth factor expression. *J Biol Chem* 2008;**283**(August (34)):23139–49.
13. Xu X, Bringas Jr P, Soriano P, Chai Y. PDGFR-alpha signaling is critical for tooth cusp and palate morphogenesis. *Dev Dyn* 2005;**232**(January (1)):75–84.
14. Fukumoto S, Miner JH, Ida H, Fukumoto E, Yuasa K, Miyazaki H, et al. Laminin alpha5 is required for dental epithelium growth and polarity and the development of tooth bud and shape. *J Biol Chem* 2006;**281**(February (8)):5008–16.
15. Yuasa K, Fukumoto S, Kamasaki Y, Yamada A, Fukumoto E, Kanaoka K, et al. Laminin alpha2 is essential for odontoblast differentiation regulating dentin sialoprotein expression. *J Biol Chem* 2004;**279**(March (11)):10286–92.
16. de Vega S, Iwamoto T, Nakamura T, Hozumi K, McKnight DA, Fisher LW, et al. TM14 is a new member of the fibulin family (fibulin-7) that interacts with extracellular matrix molecules and is active for cell binding. *J Biol Chem* 2007;**282**(October (42)):30878–88.
17. Chai Y, Bringas Jr P, Mogharei A, Shuler CF, Slavkin HC. PDGF-A and PDGFR-alpha regulate tooth formation via autocrine mechanism during mandibular morphogenesis in vitro. *Dev Dyn* 1998;**213**(December (4)):500–11.
18. Robbins JR, McGuire PG, Wehrle-Haller B, Rogers SL. Diminished matrix metalloproteinase 2 (MMP-2) in ectomesenchyme-derived tissues of the Patch mutant mouse: regulation of MMP-2 by PDGF and effects on mesenchymal cell migration. *Dev Biol* 1999;**212**(August (2)):255–63.

19. Nakao K, Itoh M, Tomita Y, Tomooka Y, Tsuji T. FGF-2 potently induces both proliferation and DSP expression in collagen type I gel cultures of adult incisor immature pulp cells. *Biochem Biophys Res Commun* 2004;**325**(December (3)):1052–9.
20. Tsuboi T, Mizutani S, Nakano M, Hirukawa K, Togari A. Fgf-2 regulates enamel and dentine formation in mouse tooth germ. *Calcif Tissue Int* 2003;**73**(November (5)): 496–501.
21. Fukumoto S, Kiba T, Hall B, Iehara N, Nakamura T, Longenecker G, et al. Ameloblastin is a cell adhesion molecule required for maintaining the differentiation state of ameloblasts. *J Cell Biol* 2004;**167**(December (5)): 973–83.

THE JOURNAL OF BIOLOGICAL CHEMISTRY VOL. 284, NO. 40, pp. 27176–27184, October 2, 2009
Printed in the U.S.A.

Critical Role of Heparin Binding Domains of Ameloblastin for Dental Epithelium Cell Adhesion and Ameloblastoma Proliferation*[S]

Received for publication, June 13, 2009, and in revised form, July 27, 2009 Published, JBC Papers in Press, July 31, 2009, DOI 10.1074/jbc.M109.033464

Akira Sonoda[‡§1], Tsutomu Iwamoto[¶1], Takashi Nakamura[¶‖], Emiko Fukumoto[¶], Keigo Yoshizaki[‡], Aya Yamada[¶], Makiko Arakaki[¶], Hidemitsu Harada[**], Kazuaki Nonaka[‡], Seiji Nakamura[§], Yoshihiko Yamada[‖], and Satoshi Fukumoto[‡¶2]

From the [‡]Section of Pediatric Dentistry, Division of Oral Health, Growth and Development, and [§]First Department of Oral and Maxillofacial Surgery, Faculty of Dental Science, Kyushu University, Fukuoka 812-8582, Japan, the [¶]Division of Pediatric Dentistry, Department of Oral Health and Development Sciences, Tohoku University Graduate School of Dentistry, Sendai 980-8575, Japan, the [‖]Craniofacial Developmental Biology and Regeneration Branch, NIDCR, National Institutes of Health, Bethesda, Maryland 20892, and the [**]Department of Oral Anatomy II, Iwate Medical Collage School of Dentistry, Morioka, Iwate 020-8505, Japan

AMBN (ameloblastin) is an enamel matrix protein that regulates cell adhesion, proliferation, and differentiation of ameloblasts. In AMBN-deficient mice, ameloblasts are detached from the enamel matrix, continue to proliferate, and form a multiple cell layer; often, odontogenic tumors develop in the maxilla with age. However, the mechanism of AMBN functions in these biological processes remains unclear. By using recombinant AMBN proteins, we found that AMBN had heparin binding domains at the C-terminal half and that these domains were critical for AMBN binding to dental epithelial cells. Overexpression of full-length AMBN protein inhibited proliferation of human ameloblastoma AM-1 cells, but overexpression of heparin binding domain-deficient AMBN protein had no inhibitory effect. In full-length AMBN-overexpressing AM-1 cells, the expression of Msx2, which is involved in the dental epithelial progenitor phenotype, was decreased, whereas the expression of cell proliferation inhibitors p21 and p27 was increased. We also found that the expression of enamelin, a marker of differentiated ameloblasts, was induced, suggesting that AMBN promotes odontogenic tumor differentiation. Thus, our results suggest that AMBN promotes cell binding through the heparin binding sites and plays an important role in preventing odontogenic tumor development by suppressing cell proliferation and maintaining differentiation phenotype through Msx2, p21, and p27.

The extracellular matrix provides structural support for cells and regulates cell proliferation, migration, differentiation, and apoptosis for tissue development and homeostasis (1). The extracellular matrix also plays a crucial role in pathological processes and diseases, such as wound healing, tumorigenesis, and cancer development (2, 3). AMBN (ameloblastin), also known as amelin and sheathlin, is a tooth-specific extracellular matrix and the most abundant non-amelogenin enamel matrix protein (4–6). AMBN is expressed primarily by ameloblasts, which are differentiated from the oral ectoderm and form a polarized single cell layer underlying the enamel matrix. In a previous study, we created *Ambn*-null mice and demonstrated that AMBN is required for cell attachment and polarization and for maintaining the differentiation state of ameloblasts and is essential for enamel formation (3). Overexpression of *Ambn* in transgenic mice causes abnormal enamel crystallite formation and enamel rod morphology (7). These results suggest that enamel formation and rod morphology are influenced by temporal and spatial expressions of AMBN and imply that the *AMBN* gene locus may be involved in the etiology of a number of cases of undiagnosed hereditary amelogenesis imperfecta (8). Further, it was reported that recombinant AMBN enhances pulpal wound healing and reparative dentine formation following pulpotomy procedures, suggesting that it functions as a signal molecule in epithelial-mesenchymal interactions (9).

We previously reported that about 20% of *Ambn*-null mice developed an odontogenic tumor of dental epithelium origin in the buccal vestibule of the maxilla (3). The epithelial cells of odontogenic tumors express enamel matrix proteins, including AMEL (amelogenin), ENAM (enamelin), and TUFT (tuftelin), but not AMBN, indicating that AMBN deficiency is probably the primary cause of tumorigenesis seen in those mice. An ameloblastoma appearing in the jaw is the most frequently encountered odontogenic tumor and is characterized by benign but locally invasive behavior with a high rate of recurrence. Since abnormal proliferation and growth of ameloblastoma cells easily destroys surrounding bony tissues, wide excision is required to treat this disorder. It is also reported that ameloblastomas rarely metastasize to other parts of the body, such as the lungs and regional lymph nodes (10, 11). Associations of AMBN mutations were reported in ameloblastomas, adenomatoid odontogenic tumors, and squamous odontogenic tumors (12). These results suggest that AMBN regulates odontogenic tumor formation.

* This work was supported, in whole or in part, by the Intramural Program of the National Institutes of Health, NIDCR (to Y. Y.). This work was also supported in part by Ministry of Education, Science and Culture of Japan Grants-in-aid for Research Fellows of the Japan Society for the Promotion of Science 17689058 and 20679006 (to S. F.).

[S] The on-line version of this article (available at http://www.jbc.org) contains supplemental Table S1 and Fig. S1.

[1] Both authors contributed equally to this work.

[2] To whom correspondence should be addressed. Fax: 81-22-717-8386; E-mail: fukumoto@mail.tains.tohoku.ac.jp.

In the present study, we investigated the mechanism of AMBN in dental epithelial cell adhesion and ameloblastoma proliferation. We found that AMBN has heparin binding domains, which are essential for AMBN binding to dental epithelial cells. We demonstrate that overexpression of recombinant AMBN inhibits proliferation of human ameloblastoma cells. This inhibition requires the heparin binding sites of AMBN and is accompanied by dysregulation of Msx2, p21, and p27. These results suggest that AMBN suppresses ameloblastoma cell proliferation by regulating cellular signaling through the heparin binding domains.

EXPERIMENTAL PROCEDURES

Expression and Purification of Recombinant Ameloblastin—The expression vector pEF6/V5-His-Topo (Invitrogen) was used to express His-tagged rat AMBN proteins, as described previously (3). The expression plasmids were transfected into COS-7 cells using Lipofectamine 2000 (Invitrogen). After 2 days, transfected cells were lysed using lysis buffer (1% Triton X-100, 10 mM Tris-HCl, pH 7.4, 150 mM BaCl, 10 mM $MgCl_2$), and His-tagged recombinant proteins were purified with a TARON purification system (Clontech), according to the manufacturer's instructions. Purified proteins were separated by SDS-PAGE and analyzed by Western blotting.

Cell Culture and Transfection—For dental epithelial cell cultures, molars from P3 mice were dissected. The molars were treated with 0.1% collagenase, 0.05% trypsin, 0.5 mM EDTA for 10 min, and the dental epithelium was separated from the dental mesenchyme. The separated dental epithelium was treated with 0.1% collagenase, 0.05% trypsin, 0.5 mM EDTA for 15 min and then transferred with a pipette up and down into culture wells. Dental epithelial cells were then selected by culturing in keratinocyte-SFM medium (Invitrogen), supplemented with epidermal growth factor and bovine pituitary extract, for 7 days to remove contaminated mesenchymal cells. Cells were then detached with 0.05% EDTA, washed with DME containing 0.1% bovine serum albumin, resuspended to a concentration of 1.0×10^5/ml, and used for cell adhesion assays. HAT-7 and SF2 cells from dental epithelium were maintained in Dulbecco's modified Eagle's medium/F-12 medium supplemented with 10% fetal bovine serum (13, 14). AM-1 cells, which were established from human ameloblastoma tissue by human papilloma virus type 16, were maintained in defined keratinocyte-SFM medium supplemented with adjunctive growth supplement (Invitrogen). COS-7 and SQUU cells were maintained in Dulbecco's modified Eagle's medium (Invitrogen) supplemented with 10% fetal bovine serum. All cells were cultured with 1% penicillin and streptomycin (Invitrogen) at 37 °C in a humidified atmosphere containing 5% CO_2. AM-1, COS-7, and SQUU cells were transiently transfected with an AMBN expression plasmid using Lipofectamine 2000 (Invitrogen) according to the manufacturer's protocol.

Cell Adhesion Assays—Cell adhesion assays were performed in 96-well round bottom microtiter plates (Immulon-2HB; Dynex Technologies, Inc.). The wells were coated overnight at 4 °C with 10 μg/ml recombinant rat AMBN, recombinant mouse AMEL (15), or laminin 10/11 (R&D systems), each diluted with PBS,[3] and blocked with 3% bovine serum albumin for 1 h at 37 °C. After washing, 10^4 cells were treated with or without heparin (Sigma), heparan sulfate (Sigma), laminin 10/11, or 5 milliunits of heparitinase (Seikagaku Co.) and then added to plates and incubated for 60 min at 37 °C. The plates were washed with PBS three times to remove unattached cells, and then attached cells were treated with 0.05% trypsin, 0.5 mM EDTA and counted under a microscope.

RNA Isolation and Reverse Transcription-PCR—Total RNA was isolated using TRIzol (Invitrogen) according to the manufacturer's protocol. First strand cDNA was synthesized at 42 °C for 90 min using oligo$(dT)_{14}$ primer with SuperScript III (Invitrogen). PCR amplification was performed using the primers listed in supplemental Table S1. The PCR products were separated on a 1.5% agarose gel. The relative expression level was deduced from a standard curve constructed using the positive control sample and normalized against the expression level of glyceraldehyde-3-phosphate dehydrogenase in each sample.

Western Blotting—Forty-eight hours after transfection with various AMBN expression vectors, cells were washed twice with 1 mM ice-cold sodium orthovanadate (Sigma) in PBS, lysed with Nonidet P-40 buffer supplemented with a proteinase inhibitor mixture (Sigma) and phenylmethanesulfonyl fluoride at 4 °C for 10 min, and centrifuged, and then the supernatants were transferred to fresh tubes. For a heparin binding assay, protein lysates were incubated with Ni^{2+}-nitrilotriacetic acid beads (Sigma) or heparin-acrylic beads (Sigma) for 12 h at 4 °C and then washed with lysis buffer three times. The cell lysates or purified proteins obtained using nickel or heparin beads were separated by 4–12% SDS-PAGE and analyzed by Western blotting. The blotted membranes were incubated with antibodies for V5-tag (Invitrogen) and AMBN (3), and signals were detected with an ECL kit (Amersham Biosciences).

Bromodeoxyuridine (BrdUrd) Incorporation and Cell Counting—For the BrdUrd incorporation assay, cells were incubated at the same cell density for 48 h after transfection with the various vectors. BrdUrd (Sigma) (10 μM) was added to the plates for 60 min, and then the cells were fixed with cold methanol for 20 min, rehydrated in PBS, and incubated for 30 min in 1.5 M HCl. After washing three times in PBS, the plates were incubated with a 1:50 dilution of fluorescein isothiocyanate-conjugated anti-BrdUrd antibody (Roche Applied Science) for 30 min at room temperature. Finally, the cells were washed in PBS three times and incubated with 10 μg/ml propidium iodide (Sigma) in PBS for 30 min at room temperature. BrdUrd-positive cells were examined under a microscope (Biozero-8000; Keyence, Japan). AM-1 cells with or without AMBN expression vector transfection were cultured with serum for 48 h and then plated into 6-well plates at a density of 1×10^4 cells/well. Cell numbers were determined using a trypan blue dye exclusion method. Cells were incubated with 10% fetal bovine serum for 0–120 h and then counted in a counting chamber. Cell count analysis was performed in tripli-

[3] The abbreviations used are: PBS, phosphate-buffered saline; BrdUrd, bromo-2′-deoxyuridine; ERM, epithelial cell rests of Malassez.

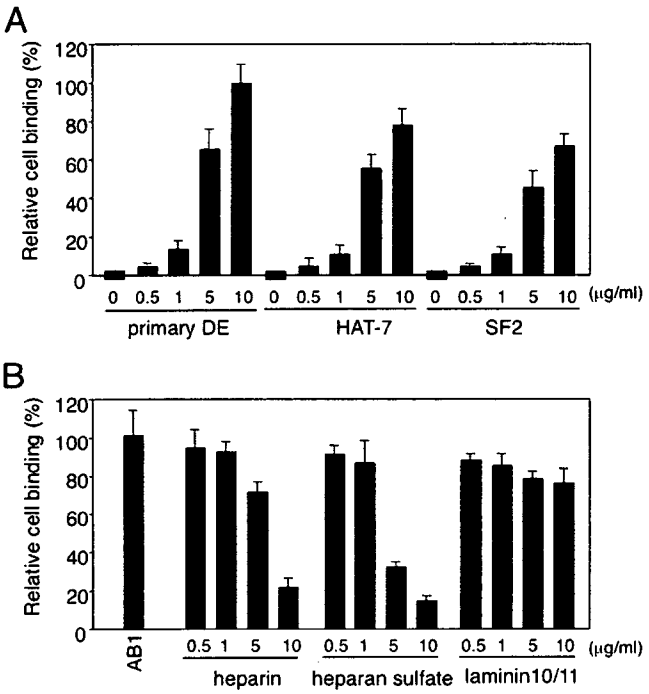

FIGURE 1. **Dental epithelial cell adhesion to recombinant AMBN and inhibition by heparin and heparan sulfate.** *A*, adhesion of primary dental epithelial cells and rat dental epithelial HAT-7 and SF2 cells to dishes coated with various amounts of full-length recombinant AMBN (AB1). *DE*, primary dental epithelial cells. *B*, inhibition of HAT-7 cell adhesion to AMBN and laminin 10/11 by heparin and heparan sulfate. Heparin and heparan sulfate inhibited cell adhesion to AMBN but not to laminin 10/11.

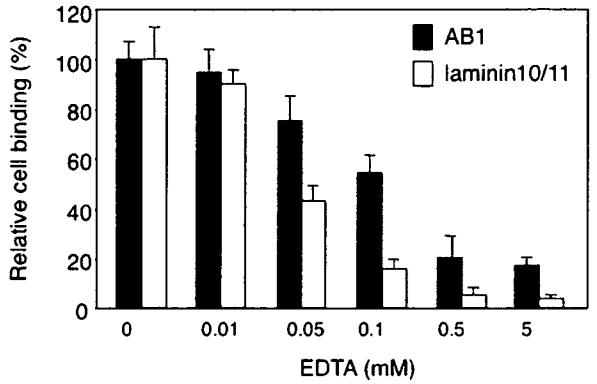

FIGURE 2. **Inhibition of cell adhesion to AMBN and laminin 10/11 by EDTA.** Adhesion of HAT-7 cells to dishes coated with full-length recombinant AMBN (AB1) and laminin 10/11 in the presence of various concentrations of EDTA. The inhibitory effect of EDTA on dental epithelial cell adhesion to AMBN was less effective than that of laminin 10/11.

cate for each time point, and the presented results are the average of 10 independent experiments.

RESULTS

AMBN Binding to Dental Epithelial Cells Is Inhibited by Heparin and Heparan Sulfate—To analyze cell adhesion to recombinant AMBN, we created V5-His-tagged recombinant AMBN (see Fig. 3*A*). The anti-V5 antibody was able to detect the recombinant protein as a specific band of about 58 kDa, which is larger than the predicted molecular size of the AMBN-V5-His fusion protein. This higher molecular weight on SDS-PAGE is due to the unconventional protein property of AMBN (16). Primary dental epithelium bound to full-length AMBN (AB1) in a dose-dependent manner, as previously reported. Further, rat dental epithelial lines HAT-7 and SF2 cells also bound to AMBN in a dose-dependent manner (Fig. 1*A*).

AMBN has a VTKG motif, which is a potential thrombospondin-like cell adhesion domain (6), also known as a heparin binding domain (17). In addition, AMBN has positively charged lysine, arginine, and histidine (KRH) amino acid-rich sequences in the middle and C-terminal regions (Fig. 3*A*), and a KRH-rich motif has been proposed as a heparin binding domain (17). We found that heparin and heparan sulfate inhibited dental epithelial cell adhesion to AB1 but not laminin 10/11 (Lam-511 and Lam-521, according to a recently proposed nomenclature) (Fig. 1*B*) (46). These findings suggest that the heparin binding domains are involved in dental epithelium cell adhesion to AMBN. Many extracellular matrix proteins bind to cells through integrins or calcium-dependent cell adhesion molecules, and this binding is inhibited in the presence of EDTA. EDTA inhibited cell adhesion to laminin 10/11, which has integrin binding regions (Fig. 2) (18). However, the inhibitory effect of EDTA on dental epithelial cell adhesion to AMBN was less effective than that of laminin 10/11 (Fig. 2). These results suggest that non-integrin-dependent cell adhesion is important for cell binding of AMBN.

Heparin Binding Domains in AMBN Critical for Heparin Binding and Cell Adhesion—To examine the significance of the potential heparin binding domains of AMBN, we prepared truncated V5-His-tagged AMBN proteins from COS-7 cells transfected with various AMBN cDNA expression vectors (Fig. 3*A*) and determined their heparin binding properties. All recombinant proteins purified by nickel bead affinity chromatography were detected by anti-V5 antibodies (Fig. 3*B*). Some proteolytic bands were observed for the AB1, AB2, AB3, and AB4 proteins, whereas the AB6 protein band was weak as compared with the others. AB1 and AB2, which have all three heparin binding domains, and AB3, which lacks the C-terminal heparin binding domain, bound equally well to heparin beads at high levels (Fig. 3*B*), whereas AB4, which has only the N-terminal heparan binding domain, bound to the beads weaker than those three proteins. AB5, which has a half-portion of the N-terminal heparan binding domain, showed substantially reduced heparin binding activity, and AB6, which lacks all three heparan binding domains, did not bind the heparan beads at all (Fig. 3*C*). These results indicate that the two N-terminal domains are required for heparin binding of AMBN.

To examine the role of the heparin binding domains in AMBN cell binding, dental epithelial cells were plated on dishes coated with purified AMBN recombinant proteins, and cell binding was measured. The AB2, AB3, and AB4 proteins had about 60% cell binding activity compared with that of AB1, and the levels for AB5 cell binding were further lower by 30% than AB1. AB6 showed little cell binding (Fig. 4*A*). Heparin inhibited cell binding of AB2 but not AB5 (Fig. 4*B*). These results suggest that AMBN has a heparin-insensitive cell binding region at the N-terminal half and a heparin-sensitive cell binding region at the C-terminal half.

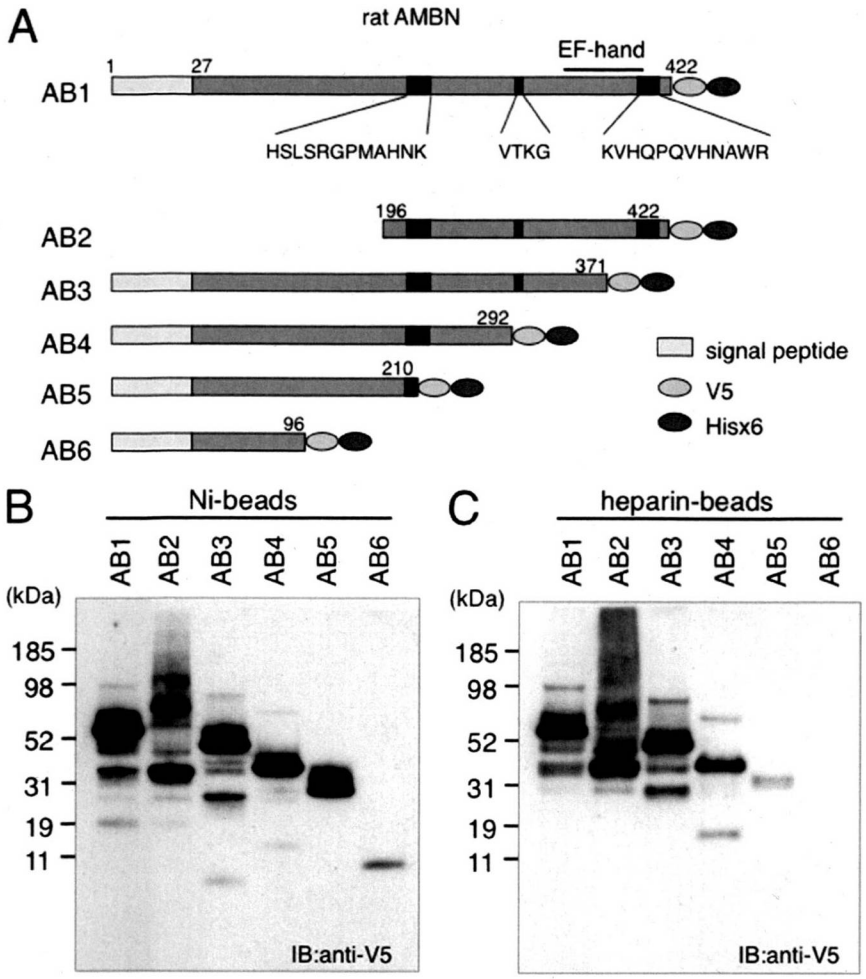

FIGURE 3. **Identification of heparin binding regions of AMBN.** *A*, creation of deletions in AMBN. All recombinant AMBN proteins have V5 and His tags at the C terminus; the amino acid sequences for potential heparin binding are shown (*black boxes*). *B*, expression of mutant AMBN proteins. An expression vector for each recombinant AMBN was transfected into COS-7 cells and was purified using Ni^{2+}-nitrilotriacetic acid beads. Purified proteins were separated by SDS-PAGE and visualized with the anti-V5 antibody. *C*, heparin binding of AMBN proteins. Each cell lysate was mixed with heparin-acrylic beads, and bound proteins were separated by SDS-PAGE and visualized with the anti-V5 antibody. AB1, AB2, and AB4 bound strongly to heparin. AB4 bound less to heparin, and AB5 had substantially reduced heparin binding. AB5 lost heparin binding.

AMBN has an EF-hand calcium binding region in the C terminus. Bioinformatic analysis suggests a conformational change in the AMBN protein in the presence of the Ca^{2+} ion (19). We found that heparin binding of AB1 containing an EF-hand motif was increased by EDTA in a dose-dependent manner, whereas heparin binding of AB4 lacking the EF-hand motif did not change by EDTA (Fig. 4, *C* and *D*). These results suggest that the EF-hand motif modulates heparin binding activity of AMBN. An internal deletion of the N-terminal heparin binding domain of AB1 (AB7) caused a small reduction in heparin and cell binding (Fig. 5, *A–C*). AB8, in which three heparin binding domains, but not the N-terminal sequence, were deleted from AB1, showed a nearly complete loss of heparin binding and weak cell binding activity (Fig. 5). Further, cells treated with heparitinase lost the ability to bind to AB1 (Fig. 5*C*), indicating that heparan sulfate on the surface of ameloblasts is important for cell binding to AMBN.

Overexpression of Full-length AMBN (AB1) but Not Heparin Binding Domain-deficient AMBN (AB5) Inhibits Proliferation of Ameloblastoma AM-1 Cell—*Ambn*-null mice develop odontogenic tumors, suggesting that AMBN may function as a tumor suppressor. AM-1 cells are an ameloblastoma cell line, which does not express AMBN (supplemental Fig. 1*A*). To identify the role of AMBN in odontogenic tumor proliferation, the AB1 expression vector was transfected into AM-1 cells. Transfected AM-1 cells expressed and secreted recombinant AMBN protein (supplemental Fig. 1*C*). AB1-overexpressing AM-1 cells showed a decrease in the number of BrdUrd-positive cells as compared with mock-transfected cells (Fig. 6, *A* and *B*). After transfection, the number of cells was counted every 24 h for 5 days and was found to be substantially decreased (Fig. 6*C*). However, overexpression of AB8 lacking the heparin binding domains did not affect cell proliferation as compared with mock-transfected cells (Fig. 6*D*). These results indicate that AMBN expression inhibits proliferation of AM-1 cells via the heparin binding domains.

To examine whether the inhibition of cell proliferation by AMBN is dependent on a cell type, the AB1 expression vector was transfected into COS-7 cells from a kidney fibroblast cell line and SQUU-B cells from a tongue squamous cell carcinoma cell line. BrdUrd incorporation was inhibited in AB1-overexpressing AM-1 cells but not in AB1- overexpressing COS-7 or SQUU-A cells (Fig. 7). Further, proliferation of AM-1 cells was inhibited when the cells were cultured on recombinant AMBN (AB1)-coated dishes but not recombinant AMEL- and laminin 10/11-coated dishes (Fig. 7*B*). These findings suggest that AMBN suppresses cell proliferation in a cell type-specific manner.

AMBN Expression Induces the Expression of p21 and p27 but Inhibits Msx2 Expression—To identify the inhibitory mechanism of proliferation of AM-1 cells by AMBN, we examined the expressions of *p21* and *p27*, *CDK* inhibitors and negative regulators of cell proliferation, and Msx2, a homeobox-containing transcription factor, which is expressed in undifferentiated ameloblasts (20) and in *Ambn*-null ameloblasts (3). Msx2 was strongly expressed in mock-transfected AM-1 cells; however, its expression was strongly inhibited by overexpression of AMBN (Fig. 8). We found that overexpression of AMBN

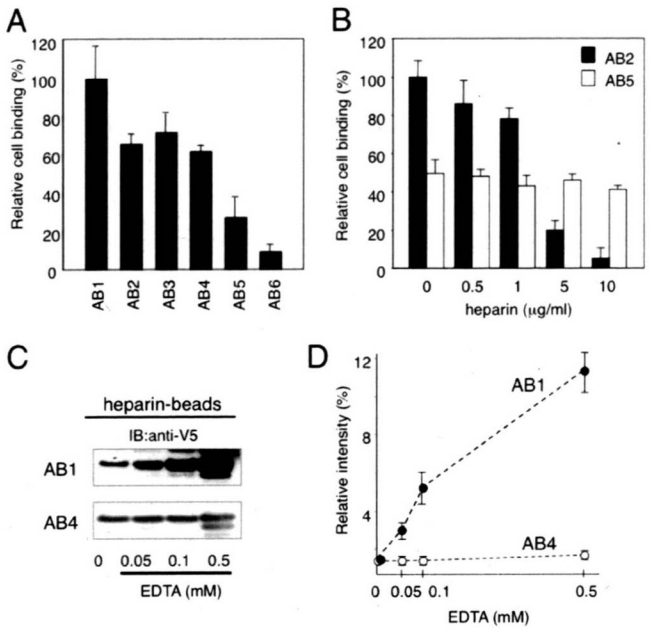

FIGURE 4. **Cell binding activity of mutant AMBN proteins.** *A*, adhesion of HAT-7 cells to dishes coated with recombinant AMBN, AB1, AB2, AB3, AB4, AB5, and AB6. Cell binding activity of AB2, AB3, and AB4 was less than that of AB1. AB5 had substantially reduced cell binding activity, and AB6 lost the binding activity. *B*, inhibition of cell binding of AB2 and AB5 by heparin. Heparin inhibited AB2 cell binding but not AB5 cell binding. *C*, effects on EDTA on heparin binding of AB1 and AB4. AB1 and AB4 were incubated with heparin-acrylic beads in the presence of various concentrations of EDTA. Bound proteins were separated with SDS-PAGE and detected by Western blotting using the anti-V5 antibody. *D*, quantitation of the intensity of the protein bands in *C*. The intensity of bands without EDTA was set at 1 for comparison. EDTA affects heparin binding of AB1 but not AB4.

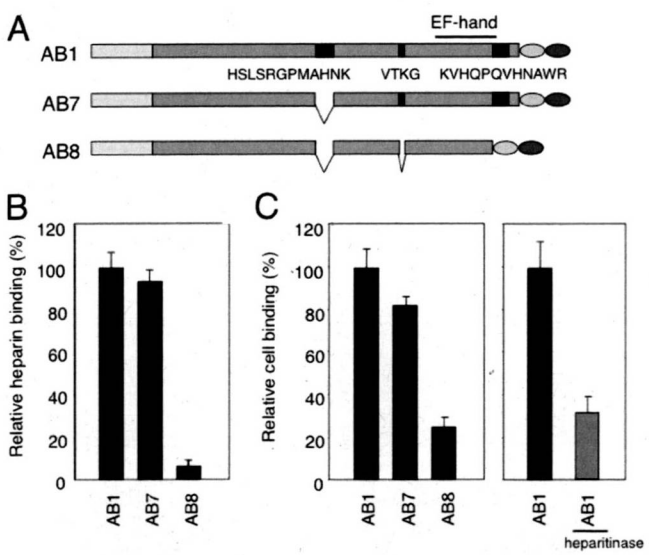

FIGURE 5. **Deletion analysis of heparin binding regions of AMBN for heparin binding and cell adhesion.** *A*, deletions of recombinant AMBN proteins. AB7 results from deletion of the first heparin binding region, and AB8 is the result of deletion of all three heparin binding regions. *B*, heparin binding of AB1, AB7, and AB8. AB7 slightly reduced heparin binding activity, but AB8 lost all activity. Heparin binding of AB1 was set at 100%. *C*, adhesion of HAT-7 cells to dishes coated with AB1, AB7, and AB8. AB7 had reduced cell binding activity. AB8 further reduced cell binding. Cells pretreated with heparitinase showed decreased binding to AB1. Cell adhesion of AB1 was set at 100% for comparison.

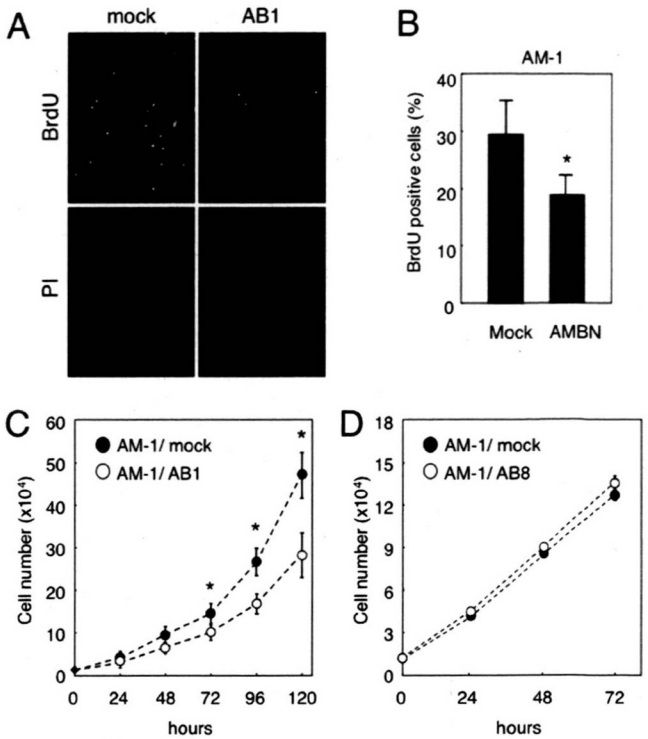

FIGURE 6. **Inhibition of proliferation of AM-1 cells by overexpression of AMBN.** *A*, AM-1 human ameloblastoma cells were transfected with a mock or AB1 expression vector and cultured for 48 h. BrdUrd was incorporated into the cells for 1 h. BrdUrd incorporation was analyzed using a fluorescence microscope. *B*, quantitation of BrdUrd-positive cells in *A*. Expression of AMBN-inhibited AM-1 proliferation. *C*, inhibition of AM-1 cell growth of by AB1 expression. AM-1 cells were transfected with mock or AB1 expression vector. The number of the cells was counted using a trypan blue exclusion method after 0–120 h of culture. *D*, no inhibitory effects of AB8 expression on AM-1 cell growth were seen. The numbers of AM-1 cells with transfection of the mock or AB8 expression vector were counted from 0 to 72 h. Statistical analysis was performed using analysis of variance (*, $p < 0.01$).

induced the expression of both *p21* and *p27*, whereas the expression of positive cell cycle regulators *CDK1*, *-4*, and *-6* was not changed (Fig. 8). These results suggest that AMBN promotes odontogenic cell differentiation and inhibits proliferation via p21 and p27 expression in a CDK-independent manner.

Overexpression of AMBN in AM-1 Cells Induces Expression of ENAM but Not AMEL—Our finding that AMBN expression inhibited *Msx2* expression suggests that AMBN promotes odontogenic cell differentiation. To better elucidate the function of AMBN in AM-1 cell differentiation, we examined whether AMBN has effects on the expression of other enamel matrix proteins. AMBN overexpression in AM-1 cells strongly induced the expression of *ENAM* mRNA (Fig. 9), whereas the expression of *AMEL* and *TUFT* was not affected. These results indicate that AMBN does not induce all enamel matrix genes but induces selectively in AM-1 cells and suggests that AMBN may serve as a suppressor of odontogenic tumors by regulating cellular signaling for differentiation and proliferation.

DISCUSSION

We previously found using *Ambn*-null mice and cell culture that AMBN is an adhesion molecule for ameloblasts and required for maintaining a single ameloblast cell layer

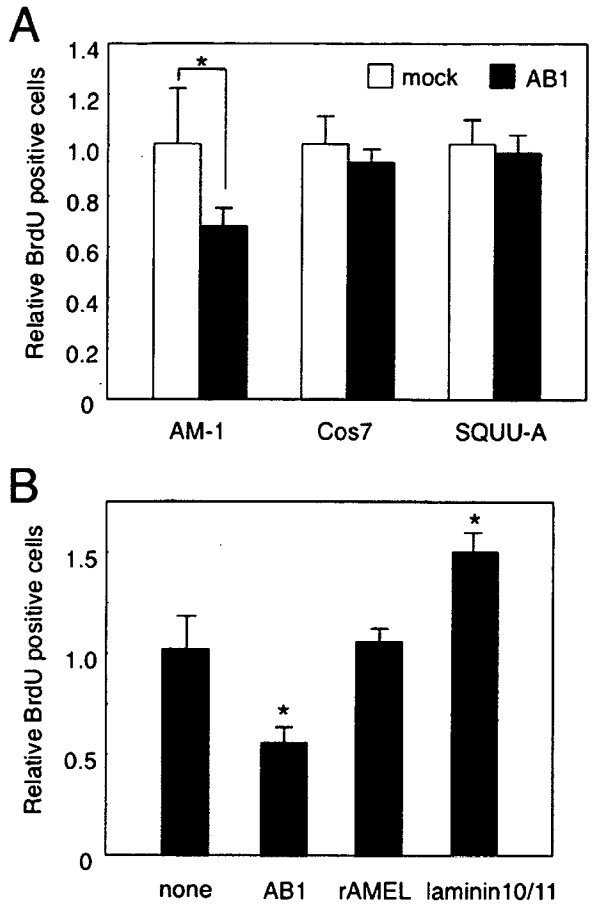

FIGURE 7. **Cell type-specific inhibition of proliferation by AMBN.** *A*, AB1. AM-1, COS-7, and SQUU-A cells were plated on dishes coated with AMBN (10 mg/ml) and cultured for 48 h. BrdUrd was incorporated into the cells for 1 h. BrdUrd-positive cells were counted. Proliferation of AM-1 cells, but not COS-7 and SQUU-A cells, was reduced on AB1 substrate. The number of BrdUrd-positive cells with mock-transfected cells was set at 100%. *B*, adhesion of AM-1 cells to dishes coated with AB1, recombinant AMEL (*rAMEL*), and laminin 10/11. The number of BrdUrd-positive cells with cells cultured on a non-coated dish was set at 100%. Statistical analysis was performed using analysis of variance (*, $p < 0.01$).

attached to the enamel matrix and the differentiation state of ameloblasts. In this paper, we identify the heparin binding domains of AMBN and demonstrate that these domains play a critical role in AMBN binding to dental epithelial cells. We also show that AMBN inhibits proliferation of human ameloblastoma cells. This inhibition is accompanied by the induction of *p21* and *p27* and *ENAM* and the reduction of *Msx2*. It was recently reported that AMBN fusion protein enhances pulpal healing and dentin formation in porcine teeth (21). In addition, AMBN promotes adhesion of periodontal ligament cells and modulates the expression of bone morphogenic protein, collagen type I, and osteocalcin (22). Those results implicate that AMBN regulates cell proliferation and differentiation through cellular signaling induced by the AMBN interaction with cells. Our finding that AMBN cell binding is mediated through the heparin binding domains suggests that AMBN interacts with heparan sulfate (HS) cell surface receptors. However, we could not detect AMBN binding to lymphoid cell lines expressing individual HS cell surface receptors, including syndecan-1, -2, and -4 (data not shown) (23). We also could not find the interaction of AMBN with glypican-1, which is expressed in ameloblasts (data not shown). Laminin is one of the heparin and integrin binding molecules. The laminin α1 chain LG4 module promotes cell attachment through syndecans and cell spreading through integrin $\alpha 2\beta 1$ (23). Active sequences in the LG4 of other laminin α chains have also been identified for cell attachment and heparin and syndecan binding (24–26). Further, Lys and Arg amino acid-rich regions of the LG4 module are important for heparin and HS binding. These regions may be similar to those of AMBN. A recent study (27) showed that laminin-sulfatide interaction modulates basement membrane assembly and regulates cellular signaling. It is possible that AMBN may bind cells through interacting with other co-receptors, including cell surface glycolipids and extracellular matrix.

Rodent AMBN contains a DGEA motif, which is a potential integrin-binding site of collagen I, and a thrombospondin-like cell adhesion motif, VTKG (6, 28). We found that recombinant full-length AMBN produced in mammalian cells binds specifically to primary dental epithelial cells but not to other cell types. Primary dental epithelial cells contain mixed epithelial cell populations, including inner dental epithelial cells, ameloblasts, stratum intermedium cells, and stellate cells. We found that ameloblasts, but not the other cell types, adhere to recombinant AMBN (3). In the present study, we showed that ameloblast cell lines HAT-7 and SF2 (Fig. 1) and ameloblastoma cell line AM-1 (data not shown) also bind to AMBN. The DGEA and VTKG sequences are conserved only in rodents, with little or no conservation of those motifs in other species, including human, pig, bovine, and caiman (28). Further, integrin expression disappears in differentiated ameloblasts, suggesting that other motifs in AMBN may be important for cell adhesion (18, 28, 29). The VTKG region is also known as a heparin binding domain. AMBN has positively charged Lys, Arg, and His amino acid-rich sequences in the middle and C-terminal regions (Fig. 3*A*), and KRH-rich motifs have been proposed as candidate heparin binding domains (17). The middle and C-terminal KRH-rich motifs in AMBN are conserved in human, rodent, and bovine cells, indicating that these domains may be important for cell binding. We found that full-length rat AMBN had a high affinity to heparin, whereas deletions of the heparin binding domains abrogated binding to heparin and resulted in reduced cell binding, indicating that VTKG and KRH-rich motifs serve as heparin and cell binding domains.

The EF-hand structure, which has a helix-loop-helix design, is the most common Ca^{2+}-binding motif (30). AMBN has an EF-hand motif in the C-terminal region, and proteolytic peptides from that region, particularly those migrating at 27 and 29 kDa, can be seen on SDS-PAGE assays of calcium binding. Previously, these peptides were identified in a direct ^{45}C-binding study (31) and by "Stain-all" solution, which is a detector of calcium-binding protein of enamel extract samples (32). In addition, a bioinfomatics model supports earlier experimental observations that AMBN is a bipolar,

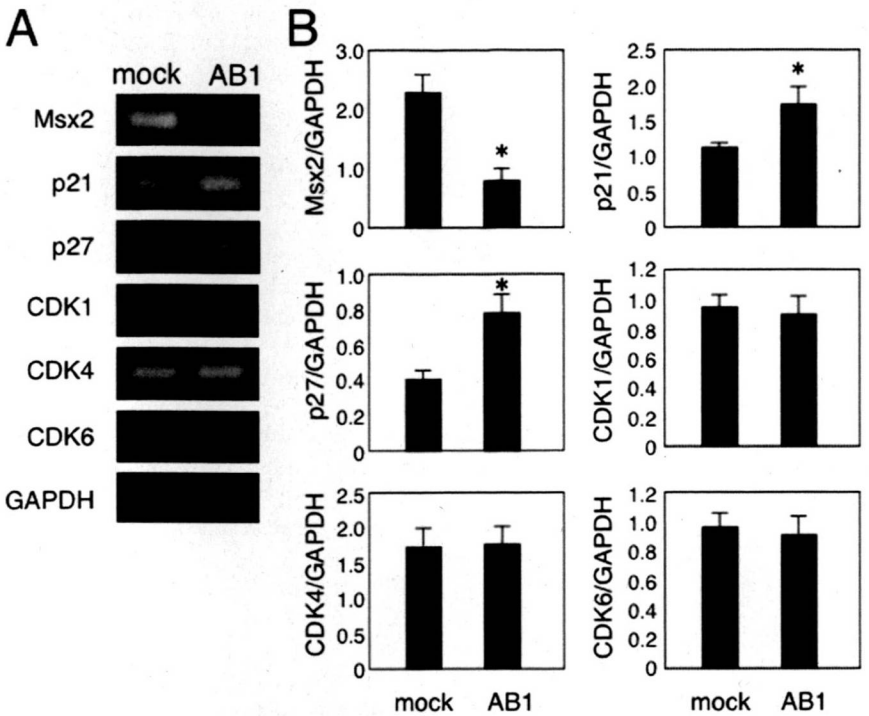

FIGURE 8. **Expression of cell cycle-regulatory genes in AMBN-overexpressing AM-1 cells.** *A*, total RNA from AM-1 cells transfected with a mock or AB1 expression vector was amplified using a semiquantitative reverse transcription-PCR method with specific primer sets. *B*, the intensity of each band was standardized with that of the glyceraldehyde-3-phosphate dehydrogenase band. *Msx2* expression was reduced, whereas expression of *p27* and *p21* was increased in AMBN-overexpressing cells. Statistical analysis was performed using analysis of variance (*, $p < 0.01$).

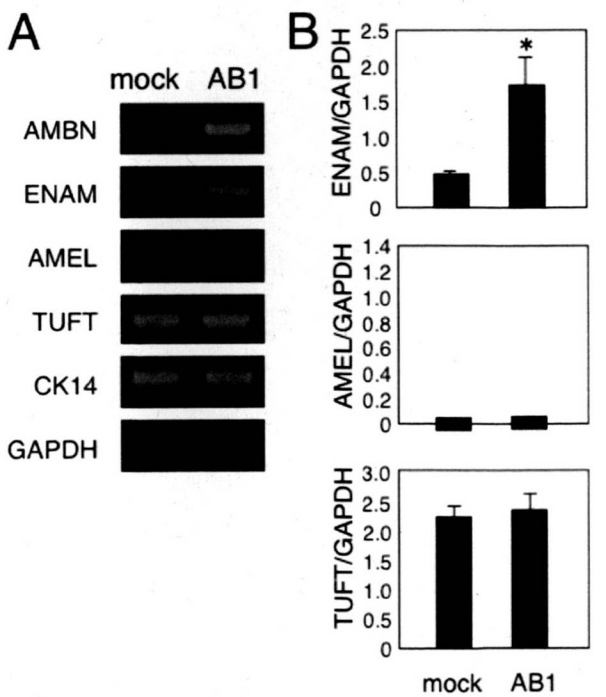

FIGURE 9. **Expression of enamel matrix proteins in AMBN-overexpressing AM-1 cells.** *A*, total RNA from AM-1 cells transfected with a mock or AB1 expression vector was amplified using a semiquantitative reverse transcription-PCR method with specific primer sets for tooth-specific genes. *B*, the intensity of the *AMBN*, *AMEL*, and *TUFT* bands was standardized with that of the glyceraldehyde-3-phosphate dehydrogenase band. *ENAM*, but not *AMEL*, was induced by AMBN overexpression. Statistical analysis was performed using analysis of variance (*, $p < 0.01$).

two-domain protein that interacts with Ca^{2+} ions. The primary structure of AMBN can be divided into two chemically and physically distinct regions: a basic N-terminal region and acidic C-terminal region. It has been speculated that the three-dimensional structure of AMBN is dramatically changed in water and in the presence of Ca^{2+} ions after molecular dynamics stimulation and energy optimization (19). Our findings agree with these reports, since AMBN heparin binding ability changed dramatically in the presence of EDTA, and this change was dependent on the EF-hand motif (Fig. 4, *C* and *D*). However, attachment of dental epithelium to AMBN did not increase in the presence of EDTA (Fig. 2), suggesting that other calcium-dependent molecules may be involved in cell binding. Further, in amelogenesis, AMBN is cleaved after secretion by several protease, including MMP-20 (33). The cleaved C-terminal half of AMBN is located near the cell surface of ameloblasts, and the N-terminal half of AMBN is present in the calcified front of enamel (34), indicating that the C-terminal region of AMBN may be important for cell binding *in vivo*. Recently, *AMBN* has been reported to appear in three different molecular sizes (37, 55, and 66 kDa) in both ameloblasts and enamel matrix during postnatal development (35). There may be various transcripts of *Ambn* that are developmentally expressed and interact with AMEL (16). Interestingly, 37-kDa AMBN containing three heparin binding domains is expressed in the early stage of ameloblast differentiation. These results indicate that the C-terminal region of AMBN is important for cell adhesion, ameloblast differentiation, and enamel nucleation.

Amelogenin and AMBN were shown to be expressed in not only ameloblasts but also odontoblasts (36). The surface of dentin has a layer of keratan sulfate rich in sulfated sialic acids and GlcNAc emanating from the dentinal tubules, which is a potent ligand for amelogenin (16). Ameloblastin may have a similar function with dentin matrix and odontoblast differentiation. Additional experiments are needed to resolve this issue.

Epithelial odontogenic tumors are histologically related to the remnants of odontogenic epithelium, which includes the dental lamina, enamel organ, and Hertwig's epithelial root sheath (37). Actively growing dental lamina is present within the jaws for a considerable time after birth, and because of the widespread presence of odontogenic epithelium, some tumors may arise from residues of those cells. AMBN is expressed by differentiated ameloblasts and also in forming Hertwig's epithelial root sheath cells and can be used as a marker of their migration (38). Previous immunohistochem-

ical studies have attempted to investigate the differentiation of neoplastic cells in odontogenic tumors; however, it was reported that AMBN, AMEL, and ENAM were not expressed in ameloblastoma cells (39, 40). *Ambn*-null mice develop odontogenic tumors of dental epithelium origin in addition to severe enamel hypoplasia. Further, because the ameloblasts disappear after eruption, tooth enamel is never replaced or repaired, and odontogenic epithelium almost completely disappears when tooth formation is completed in those mice. However, it is known that discrete clusters of odontogenic epithelial cells remain in the periodontal ligament as the epithelial cell rests of Malassez (ERM) (41). Although the function of ERM cells is still unclear, it is considered that a number of odontogenic tumors arise from them (41, 42). Recently, it was reported that ERM cells express AMBN but not AMEL or ENAM (43). It was also reported that *AMBN* gene mutations are associated with odontogenic tumors, including ameloblastomas (12, 44). In the study, we showed that AM-1 cells do not express AMBN, but overexpression of AMBN suppresses proliferation of AM-1 cells. Taken together, we speculate that AMBN functions as an odontogenic tumor suppressor.

Msx2, a homeobox-containing transcription factor, was previously shown to be expressed in undifferentiated ameloblasts, whereas it is down-regulated in differentiated ameloblasts (20). In *Ambn*-null ameloblasts, an abnormal up-regulation of Msx2 was observed (3), suggesting that AMBN inhibits the expression of Msx2 in normal tooth development. Our finding that AMBN transfection dramatically reduced Msx2 expression supports the notion that AMBN negatively regulates Msx2 expression. It has been suggested that Msx homeobox genes inhibit differentiation through up-regulation of cyclin D1 (45). In AMBN-transfected AM-1 cells, the cyclin-dependent kinase inhibitors *p21* and *p27* were up-regulated, whereas the expressions of *CDK1*, *-4*, and *-6* were not changed. Thus, down-regulation of *Msx2* and up-regulation of *p21* and *p27* by AMBN expression probably cause reduced proliferation of AM-1 cells. Further, the overexpression of AMBN lacking three heparin binding domains did not inhibit proliferation of AM-1 cells, suggesting the crucial role of the heparin binding domains of AMBN for the inhibition of AM-1 proliferation. It is conceivable that AMBN induces cellular signaling for these cellular changes by its interaction with AM-1 cells.

REFERENCES

1. Damsky, C. H., and Werb, Z. (1992) *Curr. Opin. Cell Biol.* **4,** 772–781
2. Arikawa-Hirasawa, E., Wilcox, W. R., Le, A. H., Silverman, N., Govindraj, P., Hassell, J. R., and Yamada, Y. (2001) *Nat. Genet.* **27,** 431–434
3. Fukumoto, S., Kiba, T., Hall, B., Iehara, N., Nakamura, T., Longenecker, G., Krebsbach, P. H., Nanci, A., Kulkarni, A. B., and Yamada, Y. (2004) *J. Cell Biol.* **167,** 973–983
4. Krebsbach, P. H., Lee, S. K., Matsuki, Y., Kozak, C. A., Yamada, K. M., and Yamada, Y. (1996) *J. Biol. Chem.* **271,** 4431–4435
5. Fong, C. D., Slaby, I., and Hammarström, L. (1996) *J. Bone Miner. Res.* **11,** 892–898
6. Cerný, R., Slaby, I., Hammarström, L., and Wurtz, T. (1996) *J. Bone Miner. Res.* **11,** 883–891
7. Paine, M. L., Wang, H. J., Luo, W., Krebsbach, P. H., and Snead, M. L. (2003) *J. Biol. Chem.* **278,** 19447–19452
8. MacDougall, M., Simmons, D., Gu, T. T., Forsman-Semb, K., Mårdh, C. K., Mesbah, M., Forest, N., Krebsbach, P. H., Yamada, Y., and Berdal, A. (2000) *Eur. J. Oral Sci.* **108,** 303–310
9. Nakamura, Y., Slaby, I., Spahr, A., Pezeshki, G., Matsumoto, K., and Lyngstadaas, S. P. (2006) *Calcif. Tissue Int.* **78,** 278–284
10. Ramadas, K., Jose, C. C., Subhashini, J., Chandi, S. M., and Viswanathan, F. R. (1990) *Cancer* **66,** 1475–1479
11. Newman, L., Howells, G. L., Coghlan, K. M., DiBiase, A., and Williams, D. M. (1995) *Br. J. Oral Maxillofac. Surg.* **33,** 47–50
12. Perdigão, P. F., Gomez, R. S., Pimenta, F. J., and De Marco, L. (2004) *Oral Oncol.* **40,** 841–846
13. Yuasa, K., Fukumoto, S., Kamasaki, Y., Yamada, A., Fukumoto, E., Kanaoka, K., Saito, K., Harada, H., Arikawa-Hirasawa, E., Miyagoe-Suzuki, Y., Takeda, S., Okamoto, K., Kato, Y., and Fujiwara, T. (2004) *J. Biol. Chem.* **279,** 10286–10292
14. de Vega, S., Iwamoto, T., Nakamura, T., Hozumi, K., McKnight, D. A., Fisher, L. W., Fukumoto, S., and Yamada, Y. (2007) *J. Biol. Chem.* **282,** 30878–30888
15. Nishiguchi, M., Yuasa, K., Saito, K., Fukumoto, E., Yamada, A., Hasegawa, T., Yoshizaki, K., Kamasaki, Y., Nonaka, K., Fujiwara, T., and Fukumoto, S. (2007) *Arch. Oral Biol.* **52,** 237–243
16. Ravindranath, H. H., Chen, L. S., Zeichner-David, M., Ishima, R., and Ravindranath, R. M. (2004) *Biochem. Biophys. Res. Commun.* **323,** 1075–1083
17. Yamada, Y., and Kleinman, H. K. (1992) *Curr. Opin. Cell Biol.* **4,** 819–823
18. Fukumoto, S., Miner, J. H., Ida, H., Fukumoto, E., Yuasa, K., Miyazaki, H., Hoffman, M. P., and Yamada, Y. (2006) *J. Biol. Chem.* **281,** 5008–5016
19. Vymetal, J., Slabý, I., Spahr, A., Vondrásek, J., and Lyngstadaas, S. P. (2008) *Eur. J. Oral Sci.* **116,** 124–134
20. Maas, R., and Bei, M. (1997) *Crit. Rev. Oral Biol. Med.* **8,** 4–39
21. Nakamura, Y., Slaby, I., Spahr, A., Pezeshki, G., Matsumoto, K., and Lyngstadaas, S. P. (2006) *Calcif. Tissue Int.* **78,** 278–284
22. Zeichner-David, M., Chen, L. S., Hsu, Z., Reyna, J., Caton, J., and Bringas, P. (2006) *Eur. J. Oral Sci.* **114,** Suppl. 1, 244–253; discussion 254–246, 381–242
23. Hozumi, K., Suzuki, N., Nielsen, P. K., Nomizu, M., and Yamada, Y. (2006) *J. Biol. Chem.* **281,** 32929–32940
24. Hoffman, M. P., Engbring, J. A., Nielsen, P. K., Vargas, J., Steinberg, Z., Karmand, A. J., Nomizu, M., Yamada, Y., and Kleinman, H. K. (2001) *J. Biol. Chem.* **276,** 22077–22085
25. Utani, A., Nomizu, M., Matsuura, H., Kato, K., Kobayashi, T., Takeda, U., Aota, S., Nielsen, P. K., and Shinkai, H. (2001) *J. Biol. Chem.* **276,** 28779–28788
26. Okazaki, I., Suzuki, N., Nishi, N., Utani, A., Matsuura, H., Shinkai, H., Yamashita, H., Kitagawa, Y., and Nomizu, M. (2002) *J. Biol. Chem.* **277,** 37070–37078
27. Li, S., Liquari, P., McKee, K. K., Harrison, D., Patel, R., Lee, S., and Yurchenco, P. D. (2005) *J. Cell Biol.* **169,** 179–189
28. Fukumoto, S., Yamada, A., Nonaka, K., and Yamada, Y. (2005) *Cells Tissues Organs* **181,** 189–195
29. Fukumoto, S., and Yamada, Y. (2005) *Connect. Tissue Res.* **46,** 220–226
30. Kobayashi, C., and Takada, S. (2006) *Biophys. J.* **90,** 3043–3051
31. Fukae, M., and Tanabe, T. (1987) *Adv. Dent. Res.* **1,** 261–266
32. Yamakoshi, Y., Tanabe, T., Oida, S., Hu, C. C., Simmer, J. P., and Fukae, M. (2001) *Arch. Oral Biol.* **46,** 1005–1014
33. Iwata, T., Yamakoshi, Y., Hu, J. C., Ishikawa, I., Bartlett, J. D., Krebsbach, P. H., and Simmer, J. P. (2007) *J. Dent. Res.* **86,** 153–157
34. Nanci, A., Zalzal, S., Lavoie, P., Kunikata, M., Chen, W., Krebsbach, P. H., Yamada, Y., Hammarström, L., Simmer, J. P., Fincham, A. G., Snead, M. L., and Smith, C. E. (1998) *J. Histochem. Cytochem.* **46,** 911–934
35. Ravindranath, R. M., Devarajan, A., and Uchida, T. (2007) *J. Biol. Chem.* **282,** 36370–36376
36. Nagano, T., Oida, S., Ando, H., Gomi, K., Arai, T., and Fukae, M. (2003) *J. Dent. Res.* **82,** 982–986
37. Melrose, R. J. (1999) *Semin. Diagn. Pathol.* **16,** 271–287
38. Zeichner-David, M., Oishi, K., Su, Z., Zakartchenko, V., Chen, L. S., Arzate, H., and Bringas, P., Jr. (2003) *Dev. Dyn.* **228,** 651–663
39. Saku, T., Okabe, H., and Shimokawa, H. (1992) *J. Oral Pathol. Med.* **21,**

113–119
40. Takata, T., Zhao, M., Uchida, T., Kudo, Y., Sato, S., and Nikai, H. (2000) *Virchows Arch.* **436,** 324–329
41. Rincon, J. C., Young, W. G., and Bartold, P. M. (2006) *J. Periodontal Res.* **41,** 245–252
42. Goldblatt, L. I., Brannon, R. B., and Ellis, G. L. (1982) *Oral Surg. Oral Med. Oral Pathol.* **54,** 187–196
43. Shinmura, Y., Tsuchiya, S., Hata, K., and Honda, M. J. (2008) *J. Cell Physiol.* **217,** 728–738
44. Toyosawa, S., Fujiwara, T., Ooshima, T., Shintani, S., Sato, A., Ogawa, Y., Sobue, S., and Ijuhin, N. (2000) *Gene* **256,** 1–11
45. Hu, G., Lee, H., Price, S. M., Shen, M. M., and Abate-Shen, C. (2001) *Development* **128,** 2373–2384
46. Aumailley, M., Bruckner-Tuderman, L., Carter, W. G., Deutzmann, R., Edgar, D., Ekblom, P., Engel, J., Engvall, E., Hohenester, E., Jones, J. C., Kleinman, H. K., Marinkovich, M. P., Martin, G. R., Mayer, U., Meneguzzi, G., Miner, J. H., Miyazaki, K., Patarroyo, M., Paulsson, M., Quaranta, V., Sanes, J. R., Sasaki, T., Sekiguchi, K., Sorokin, L. M., Talts, J. F., Tryggvason, K., Uitto, J., Virtanen, I., von der Mark, K., Wewer, U. M., Yamada, Y., and Yurchenco, P. D. (2005) *Matrix Biol.* **24,** 326–332

Journal of Dental Research
http://jdr.sagepub.com

Synergistic Roles of Amelogenin and Ameloblastin

J. Hatakeyama, S. Fukumoto, T. Nakamura, N. Haruyama, S. Suzuki, Y. Hatakeyama, L. Shum, C. W. Gibson, Y. Yamada and A. B. Kulkarni

J DENT RES 2009; 88; 318
DOI: 10.1177/0022034509334749

The online version of this article can be found at:
http://jdr.sagepub.com/cgi/content/abstract/88/4/318

Published by:
SAGE
http://www.sagepublications.com

On behalf of:
International and American Associations for Dental Research

RESEARCH REPORTS
Biological

J. Hatakeyama[1], S. Fukumoto[2], T. Nakamura[2], N. Haruyama[1], S. Suzuki[1], Y. Hatakeyama[3], L. Shum[3], C. W. Gibson[4], Y. Yamada[2], and A. B. Kulkarni[1]*

[1]Functional Genomics Section and [2]Molecular Biology Section, Laboratory of Cell and Developmental Biology, National Institute of Dental and Craniofacial Research, and [3]Cartilage Biology and Orthopedics Branch, National Institute of Arthritis and Musculoskeletal and Skin Diseases, National Institutes of Health, 30 Convent Dr., MSC 4395, Bethesda, MD 20892, USA; and [4]Department of Anatomy and Cell Biology, University of Pennsylvania School of Dental Medicine, Philadelphia, PA 19104, USA; *corresponding author, ak40m@nih.gov

J Dent Res 88(4):318-322, 2009

Synergistic Roles of Amelogenin and Ameloblastin

ABSTRACT

Amelogenin and ameloblastin, the major enamel matrix proteins, are important for enamel mineralization. To identify their synergistic roles in enamel development, we generated *Amel* $X^{-/-}$/*Ambn*$^{-/-}$ mice. These mice showed additional enamel defects in comparison with *Amel* $X^{-/-}$ or *Ambn*$^{-/-}$ mice. In 7-day-old *Amel* $X^{-/-}$/*Ambn*$^{-/-}$ mice, not only was the ameloblast layer irregular and detached from the enamel surface, as in *Ambn*$^{-/-}$, but also, the enamel width was significantly reduced in the double-null mice as compared with *Amel* $X^{-/-}$ or *Ambn*$^{-/-}$ mice. Proteomic analysis of the double-null teeth revealed increased levels of RhoGDI (Arhgdia), a Rho-family-specific guanine nucleotide dissociation inhibitor, which is involved in important cellular processes, such as cell attachment. Both *Amel* $X^{-/-}$/*Ambn*$^{-/-}$ mice and *Ambn*$^{-/-}$ mice displayed positive staining with RhoGDI antibody in the irregularly shaped ameloblasts detached from the matrix. Ameloblastin-regulated expression of RhoGDI suggests that Rho-mediated signaling pathway might play a role in enamel formation.

KEY WORDS: enamel, amelogenin, ameloblastin, knockout mice, RhoGDI (Arhgdia).

DOI: 10.1177/0022034509334749

Received August 25, 2008; Last revision January 8, 2009; Accepted January 12, 2009

A supplemental appendix to this article is published electronically only at http://jdr.sagepub.com/supplemental.

INTRODUCTION

Dental enamel is the most highly mineralized tissue in the body, and is formed as a result of mineralization of enamel matrices secreted by ameloblasts. Ameloblasts secrete several enamel matrix proteins, such as amelogenins, ameloblastin, and enamelin. These enamel matrix proteins are processed and degraded by proteases such as MMP20 and KLK4 during enamel mineralization (Bartlett *et al.*, 1996; Simmer *et al.*, 1998). The highly orchestrated secretion of enamel matrix proteins and their proper degradation are critical for normal enamel formation.

The amelogenin proteins are highly conserved across species, and constitute 90% of the enamel organic matrix. Based on the results from our study of *Amel* $X^{-/-}$ mice, amelogenins play an important role in enamel biomineralization (Gibson *et al.*, 2001; Hatakeyama *et al.*, 2003). In the *Amel* $X^{-/-}$ mice, ameloblast differentiation was relatively normal, but an abnormally thin enamel layer was formed (Gibson *et al.*, 2001, 2005).

It was concluded that amelogenins are essential for well-organized hydroxyapatite prism formation and elongation during enamel development, and for producing normal enamel thickness, but not for the initiation of enamel formation. Our recent studies on transgenic mice, which express the most abundant amelogenin form, M180, in the amelogenin null background, demonstrated that M180 could significantly rescue the enamel defects of the amelogenin null mice (Li *et al.*, 2008). Self-assembly of amelogenin proteins into nanospheres has been recognized as a key factor in controlling the orientation and elongated growth of crystals during the mineralizing process in enamel (Du *et al.*, 2005). Transgenic mice that express an amelogenin protein with a mutation either at the N or C terminus showed that the N-terminal domain of amelogenin might be involved in the formation of nanospheres (Paine *et al.*, 2003a), whereas the C-terminal region could contribute to stability and homogeneity in sizes of nanospheres, preventing mineral crystal fusion to form larger structures prematurely (Moradian-Oldak and Goldberg, 2005; Moradian-Oldak *et al.*, 2006). In addition, we have recently reported amelogenin's function for osteoclast differentiation in periodontal ligament tissue (Hatakeyama *et al.*, 2006).

Ameloblastin, also known as amelin or sheathlin, is an enamel-specific glycoprotein, which is the most abundant non-amelogenin enamel matrix protein (Cerný *et al.*, 1996; Krebsbach *et al.*, 1996; Fong *et al.*, 1998), and serves as a cell adhesion molecule for ameloblasts, but not for dental epithelial cells (Fukumoto *et al.*, 2004, 2005). Ameloblastin expression in ameloblasts peaks at the secretory stage and diminishes at the maturation stage. Transgenic mice overexpressing ameloblastin in ameloblasts have impaired enamel structures, suggesting the importance of normal levels of ameloblastin in enamel formation (Paine *et al.*, 2003b). Furthermore, in *Ambn*$^{-/-}$ mice, the dental epithelium differentiates into enamel-secreting ameloblasts, but the cells detach from the

matrix surface at the secretory stage and lose polarity. In ameloblasts of *Ambn*$^{-/-}$ teeth, the expression of amelogenins is reduced to about 20% of that of *Ambn*$^{+/+}$ teeth, while other enamel matrix proteins are expressed at nearly normal levels (Fukumoto *et al.*, 2004). These results suggested that ameloblastin is essential in maintaining normal ameloblast differentiation and attachment to the enamel matrix. Thus, the cellular functions of amelogenin and ameloblastin are apparently distinct, and in this paper we report potential synergistic functions of these 2 enamel proteins.

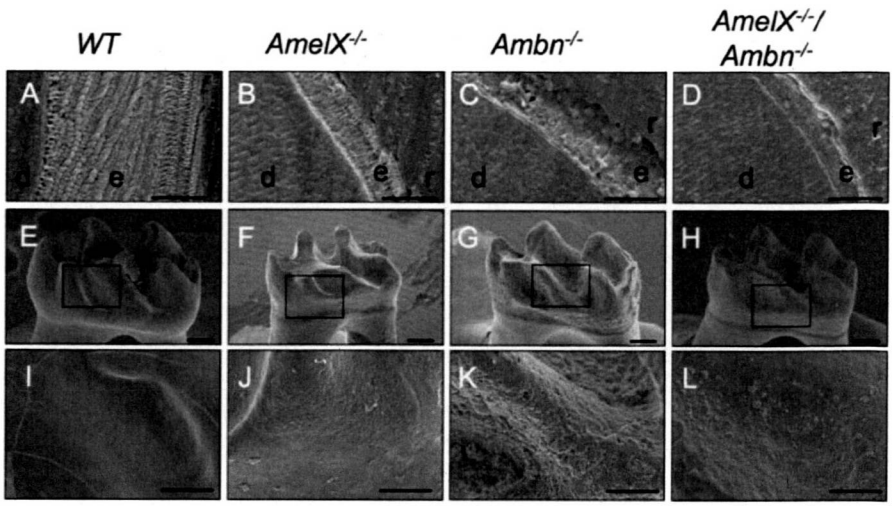

Figure 1. Scanning electron microscopy analysis of teeth from *Amel X*$^{-/-}$, *Ambn*$^{-/-}$, *Amel X*$^{-/-}$/*Ambn*$^{-/-}$, and wild-type mice. **(A-D)** Incisors from the 6-week-old mutant and wild-type mice; the enamel (e) in junction with dentin (d) is shown. Note the thin aprismatic structure in *Amel X*$^{-/-}$ mice **(B).** The enamel width of *Amel X*$^{-/-}$/*Ambn*$^{-/-}$ **(D)** mice markedly reduced as compared with that of the *Ambn*$^{-/-}$ mice **(C). (E-L)** Molars of the 6-week-old wild-type and mutant mice; note the small crown size of *Amel X*$^{-/-}$ mice **(F)** and the double-mutant **(H).** The enamel from *Amel X*$^{-/-}$(F), *Ambn*$^{-/-}$ **(G)**, and *Amel X*$^{-/-}$/*Ambn*$^{-/-}$ **(H)** appeared abnormal as compared with that in the wild-type mice (E). **(I-L)** Teeth from all 3 mutant mice mimic the amelogenesis imperfecta phenotype. *Amel X*$^{-/-}$/*Ambn*$^{-/-}$ enamel appeared less cobbled as compared with *Ambn*$^{-/-}$ enamel. Bars in A-D = 50 μm; bars in E-L = 250 μm. e, enamel; d, dentin; r, resin.

MATERIALS & METHODS

Amel X$^{-/-}$/*Ambn*$^{-/-}$ Mice

Targeted disruption of amelogenin (*Amel X*) and ameloblastin (*Ambn*) genes has been described previously (Gibson *et al.*, 2001; Fukumoto *et al.*, 2004). *Amel X*$^{-/-}$ mice were mated with *Ambn*$^{-/-}$ mice to generate double-heterozygous mice, which were interbred to generate *Amel X*$^{-/-}$/*Ambn*$^{-/-}$ mice. (Detailed information on generation and genotyping is described in the online Appendix and Appendix Fig. 1.) Mutant mice were initially analyzed in a C57BL/6 × 129/SvEv mixed genetic background and later in an enriched C57BL/6 background by being back-crossed 4 x with C57BL/6 mice. Standard NIH guidelines were followed for housing, feeding, and breeding the mice. These studies were carried out with the approval of the NIDCR Animal Care and Use Committee.

Scanning Electron Microscopic (SEM) Analyses of Incisors and Molars

Incisors and molars from wild-type and mutant mice were coated with gold and photographed by scanning electron microscopy at 20 kV (Jeol JSM T330A, Jeol, Inc., Peabody, MA, USA), and energy-dispersive spectroscopy (Kevex X-ray, Scotts Valley, CA, USA).

To observe the enamel crystals, we embedded the specimens in epoxy resin, cut them with an ISOMET low-speed saw (Buehler, Lake Bluff, IL, USA), treated them with 40% phosphoric acid for 10 sec and 10% sodium hypochlorite for 30 sec, and then coated them with gold.

Preparation of Tissue Sections and Immunohistochemistry

Post-natal (P) days 1 (P1) and 7 (P7) mouse skulls were dissected and fixed with 4% paraformaldehyde in phosphate-buffered saline (PBS) for 16 hrs at 4°C. Tissues were decalcified with 250 mM EDTA/PBS and embedded in paraffin for paraffin sections or in OCT compound (Sakura Finetechnical Co., Torrance, CA, USA) for frozen sectioning. Frozen sections were cut at 8-μm intervals on a cryostat (2800 Frigocut, Leica Inc., Wetzlar, Germany). Paraffin sections were cut at 5-μm intervals on a microtome (RM2155, Leica Inc.). For detailed morphological analysis, sections were stained with hematoxylin and eosin Y (Sigma, St. Louis, MO, USA). Frozen sections were immunostained for RhoGDI with goat polyclonal antibodies against mouse RhoGDI (Santa Cruz Biotechnology, Santa Cruz, CA, USA) overnight at 4°C at a dilution of 1:100. After being washed with PBS, the sections were incubated with peroxidase-conjugated mouse antibodies against goat IgG (Vector Laboratories, Burlingame, CA, USA), treated with diaminobenzidine substrate, and counterstained with hematoxylin for light microscopy. For control, frozen sections were incubated with secondary antibody only.

RESULTS

Defective Enamel Formation in *Amel X*$^{-/-}$/*Ambn*$^{-/-}$ Mice

SEM analysis of incisors revealed hypoplastic enamel and a lack of prism pattern in *Amel X*$^{-/-}$, *Ambn*$^{-/-}$, and *Amel X*$^{-/-}$/*Ambn*$^{-/-}$ mice that is the hallmark of organized mineral crystals in normal enamel (Figs. 1A-1D). Enamel width was much thinner in *Amel X*$^{-/-}$/*Ambn*$^{-/-}$ mice as compared with that in *Amel X*$^{-/-}$ and *Ambn*$^{-/-}$ mice. As in *Ambn*$^{-/-}$ mice, flat plate-like structures extended perpendicularly from the enamel surface to the dentin enamel junction in *Amel X*$^{-/-}$/*Ambn*$^{-/-}$ mice (Figs. 1C, 1D). The enamel surfaces appeared cobbled in both *Amel X*$^{-/-}$ (Fig. 1J) and *Ambn*$^{-/-}$ (Fig. 1K) mice. However, in *Amel X*$^{-/-}$/*Ambn*$^{-/-}$ mice, the molar surfaces appeared less cobbled than in *Amel X*$^{-/-}$ and *Ambn*$^{-/-}$ mice (Fig. 1L). Elemental

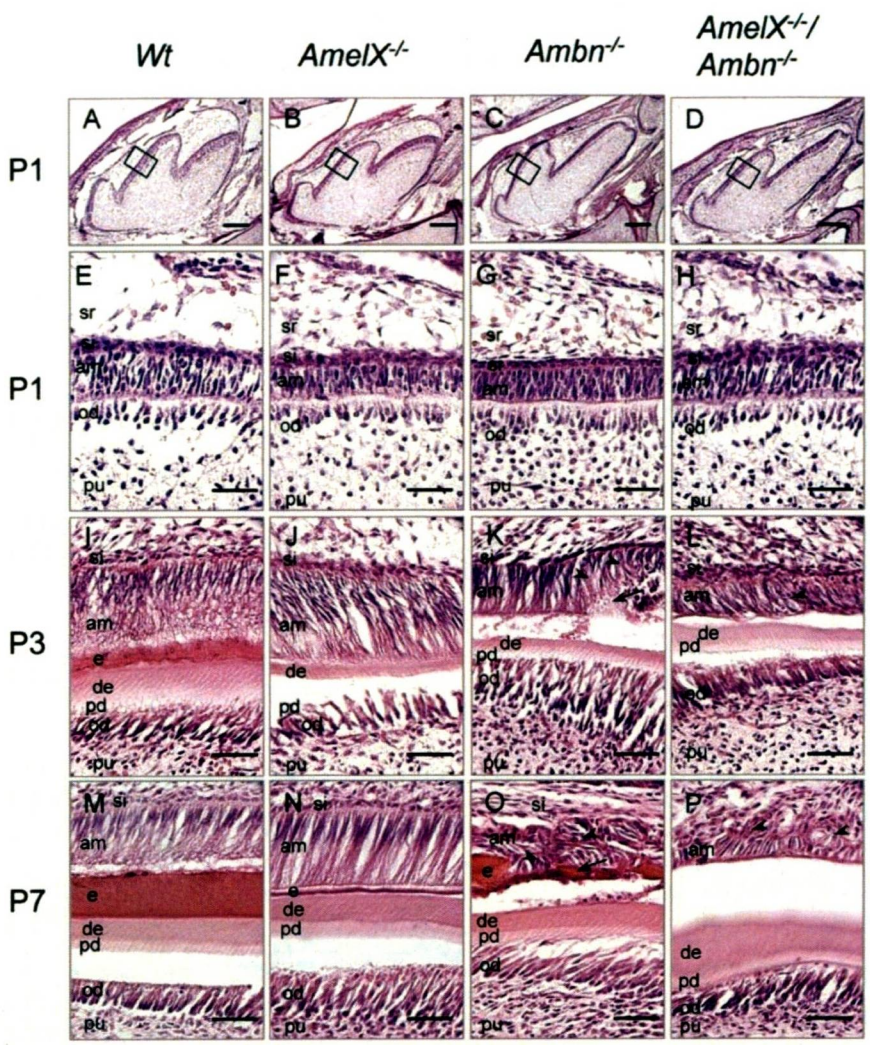

Figure 2. Histological analysis of teeth from the wild-type, *Amel X*$^{-/-}$, *Ambn*$^{-/-}$, and *Amel X*$^{-/-}$/*Ambn*$^{-/-}$ mice. Hematoxylin-eosin staining of the sagittal sections of the mandibular first molars of P1 **(A-H)**, P3 **(I-L)**, and P7 **(M-P)** wild-type and mutant mice: wild-type **(A,E,I,M)**, *Amel X*$^{-/-}$ **(B,F,J,N)**, *Ambn*$^{-/-}$ **(C,G,K,O)**, and *Amel X*$^{-/-}$/*Ambn*$^{-/-}$ mice **(D,H,L,P)**. P3 and P7 *Ambn*$^{-/-}$ ameloblasts display multiple layers containing abnormal calcified structures (Figs. 2K and 2O, arrows). *Amel X*$^{-/-}$/*Ambn*$^{-/-}$ ameloblasts also form multiple layers; however, they do not contain the calcified structures (Figs. 2L and 2P, arrowhead). am, ameloblast; si, stratum intermedium; e, enamel; pd, predentin; de, dentin; od, odontoblast; pu, pulp; sr, stellate reticulum. Bars in A-D = 500 μm; bars in E-P = 50 μm.

analysis indicated that the composition was similar to that of hydroxyapatite, indicating a normal formation of mineral in the absence of the amelogenin and ameloblastin proteins. The Ca/P molar ratio was also not significantly different in the teeth of all null mice and the WT controls (almost 1.5; data not shown).

Unlike Ambn$^{-/-}$ Ameloblasts, *Amel X*$^{-/-}$/*Ambn*$^{-/-}$ Ameloblasts Do Not Develop Calcified Nodules

In early stages of molar development up to P1, no differences were observed in either shape or size of the tooth buds of WT, *Amel X*$^{-/-}$, *Ambn*$^{-/-}$, and *Amel X*$^{-/-}$/*Ambn*$^{-/-}$ mice (Figs. 2A-2D). At P1, dentin formation of molars had begun, and dental epithelium had started to elongate and polarize with the apical nuclear localization in all of these mice (Figs. 2E-2H). Thus, cellular organization of ameloblasts and odontoblasts was similar in these mice at the pre-secretory stage. However, at P3, ameloblasts of *Ambn*$^{-/-}$ and *Amel X*$^{-/-}$/*Ambn*$^{-/-}$ mice started to detach from the matrix layer and lost the cell polarity with the centralized nuclear localization (Figs. 2K, 2L), whereas normal ameloblasts were polarized, elongated, and formed an enamel matrix in WT and *Amel X*$^{-/-}$ mice (Figs. 2I, 2J). At P7, *Ambn*$^{-/-}$ and *Amel X*$^{-/-}$/*Ambn*$^{-/-}$ ameloblasts completely lost their polarity (short and round) and accumulated to form a multilayered structure (Figs. 2O, 2P, arrowhead), in contrast to the single layer of WT and *Amel X*$^{-/-}$ ameloblasts (Figs. 2M, 2N). Interestingly, *Ambn*$^{-/-}$ ameloblasts contained calcified nodules (Fig. 2O, arrow), but *Amel X*$^{-/-}$/*Ambn*$^{-/-}$ cells did not (Fig. 2P).

Increased RhoGDI Expression in *Amel X*$^{-/-}$/*Ambn*$^{-/-}$ Ameloblasts

We utilized proteomic analysis to identify 24-kDa-size protein, which was increased in *Amel X*$^{-/-}$/*Ambn*$^{-/-}$ ameloblasts (Appendix Fig. 2). Using MALDI analysis, we identified this protein as RhoGDI. For further analysis of RhoGDI expression patterns in developing mouse molars, we carried out immunohistochemical analysis. At P1, weak RhoGDI expression was observed in ameloblasts and odontoblasts of the WT, *Amel X*$^{-/-}$, *Ambn*$^{-/-}$, and *Amel X*$^{-/-}$/*Ambn*$^{-/-}$ mice (Figs. 3A-3D). However, at P7, the ameloblasts of WT and *Amel X*$^{-/-}$ mice had no noticeable RhoGDI expression (Figs. 3E, 3F), whereas irregularly shaped ameloblasts in *Ambn*$^{-/-}$ and *Amel X*$^{-/-}$/*Ambn*$^{-/-}$ mice showed sustained expression of RhoGDI (Figs. 3G, 3H). Calcified nodules were also detected adjacent to the irregular ameloblast layer in *Ambn*$^{-/-}$ mice (Fig. 3G, arrow), but not in *Amel X*$^{-/-}$/*Ambn*$^{-/-}$ mice. We also noted increased expression of RhoGDI in the lower first molars of the 7-day-old *Amel X*$^{-/-}$/*Ambn*$^{-/-}$ mice by RT-PCR (Appendix Fig. 3).

DISCUSSION

To delineate potential synergistic roles of amelogenins and ameloblastin, we analyzed teeth from the wild-type, *Amel X*$^{-/-}$,

Ambn$^{-/-}$, and *Amel X*$^{-/-}$/*Ambn*$^{-/-}$ mice. Our analysis revealed that the *Amel X*$^{-/-}$/*Ambn*$^{-/-}$ mice displayed additional enamel defects. As compared with the *Amel X*$^{-/-}$ and *Ambn*$^{-/-}$ mice, enamel width was markedly reduced in *Amel X*$^{-/-}$/ *Ambn*$^{-/-}$ mice. Although ameloblast morphology was similar in *Ambn*$^{-/-}$ and *Amel X*$^{-/-}$/ *Ambn*$^{-/-}$ mice, calcified nodules observed in *Ambn*$^{-/-}$ ameloblasts were absent in the double-null ameloblasts. These additional defects in *Amel X*$^{-/-}$/*Ambn*$^{-/-}$ ameloblasts suggest a possible synergism in the cellular functions of amelogenins and ameloblastin.

Surprisingly, *Amel X*$^{-/-}$/*Ambn*$^{-/-}$ mice still showed a very thin layer of enamel, in spite of the lack of the 2 most abundant ECM proteins secreted by ameloblasts to form normal enamel. We found that enamelin was still expressed in the *Amel X*$^{-/-}$/*Ambn*$^{-/-}$ teeth (based on our RT-PCR analysis; data not shown). The enamelin gene (ENAM) has also been implicated in human amelogenesis imperfecta (Kim *et al.*, 2005). *Enam*$^{-/-}$ mice did not form normal enamel, because of the lack of mineralization at the secretory surfaces of the ameloblasts (Hu *et al.*, 2008). In addition, ENAM point mutation resulted in the phenotype resembling amelogenesis imperfecta (Masuya *et al.*, 2005). Therefore, it is possible that enamelin might be involved in enamel formation in the *Amel X*$^{-/-}$/*Ambn*$^{-/-}$ mice. In addition to enamelin, other ECM proteins might play a role in enamel formation in these mice, and their identification will require further studies. We had previously reported that amelogenins are involved in osteoclast differentiation in PDL cells, and furthermore, one can speculate that its lack in the double-null mice might contribute in some way to the formation of thinner enamel. Interestingly, SEM analysis of molars and incisors indicated smoother enamel in the *Amel X*$^{-/-}$/*Ambn*$^{-/-}$ mice as compared with *Ambn*$^{-/-}$ enamel. This phenotypic difference can be possibly attributed to the presence of irregular calcified nodules in *Ambn*$^{-/-}$ ameloblasts, and one can speculate that these nodules are formed because of the residual amelogenin in these mice (Fukumoto *et al.*, 2004).

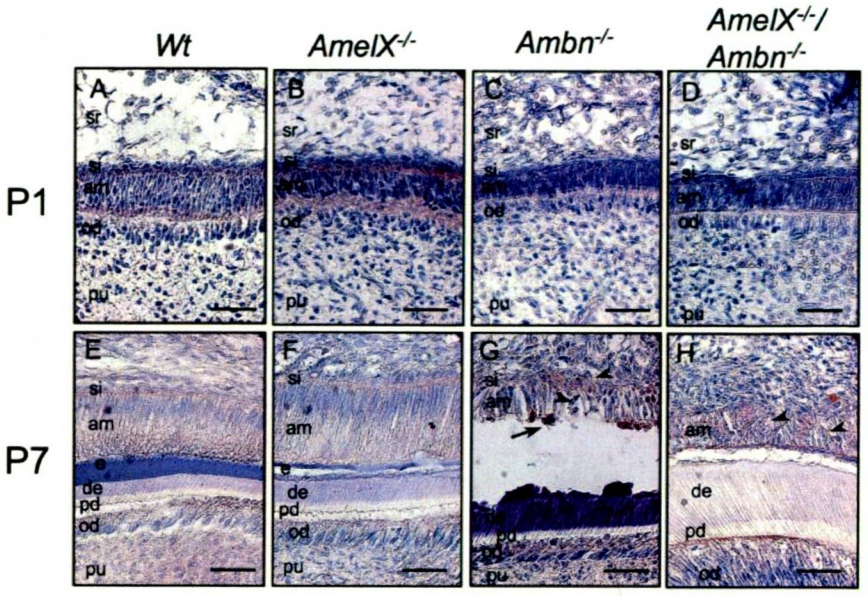

Figure 3. RhoGDI expression in the ameloblasts of the wild-type, *Amel X*$^{-/-}$, *Ambn*$^{-/-}$, and *Amel X*$^{-/-}$/ *Ambn*$^{-/-}$ mice. Sagittal sections of the incisors from the wild-type **(A,E)**, *Amel X*$^{-/-}$ **(B,F)**, *Ambn*$^{-/-}$ **(C,G)**, and *Amel X*$^{-/-}$/*Ambn*$^{-/-}$ mice **(D,H)** were stained with the RhoGDI antibody as described in MATERIALS & METHODS. Note positive staining in the detached ameloblasts of *Ambn*$^{-/-}$ **(C,G)** and *Amel X*$^{-/-}$/ *Ambn*$^{-/-}$ mice **(D,H)**. Bars = 50 μm. am, ameloblast; od, odontoblast; pu, pulp; si, stratum intermedium; e, enamel; d, dentin; pd, predentin.

Our proteomic studies identified an increased protein level of RhoGDI (Arhgdia) in *Amel X*$^{-/-}$/*Ambn*$^{-/-}$ teeth. RhoGDI, a Rho-family-specific guanine nucleotide dissociation inhibitor, forms a tight complex with Rho GTPases and inactivates Rho GTPases function as a cytosolic molecule. Reduced expression or inactivation of RhoGDIs releases Rho GTPases from the complex and translocates Rho GTPases into the membrane for activation of Rho signaling pathways (Takai *et al.*, 1995). Rho GTPases such as Rho, Rac, and Cdc42 are known to regulate assembly of filamentous actin (F-actin) and the organization of the actin cytoskeleton, and the regulation of gene transcription, cell cycle, microtubule dynamics, vesicle transport, and numerous enzymatic activities. In the wild-type teeth, RhoGDI was expressed in undifferentiated dental epithelium, but its expression was down-regulated in the secretory stage of ameloblasts. During tooth development, protein expression of RhoGDI is not altered at the early stage in *Amel X*$^{-/-}$, *Ambn*$^{-/-}$, and *Amel X*$^{-/-}$/ *Ambn*$^{-/-}$ ameloblasts. However, in later stages, when cells continue to proliferate and form multicellular layers in *Amel X*$^{-/-}$/ *Ambn*$^{-/-}$ mice, RhoGDI expression is increased. The Rho signaling pathways in murine ameloblasts are known to induce F-actin product (Li *et al.*, 2005). F-actin-rich regions have been described, and these include Tomes' process, distal terminal webs, and distal ends of ruffled or smooth-ended ameloblasts in rat incisors (Nishikawa and Kitamura, 1986).

Interestingly, the human *Amel X* gene has been shown to reside in a "nested" gene structure within intron 1 of the *ARHGAP6* gene that encodes Rho GAP, which regulates RhoA activity (Hall and Nobes, 2000; Prakash *et al.*, 2005). In some cases, expression of nested and host genes is simultaneously up- and down-regulated by common regulatory elements (Peters and Ross, 2001). It is possible that the expression of *Amel X* and *ARHGAP6* genes might be similarly regulated. Rho is recognized as a molecular switch (Hall and Nobes, 2000), which normally cycles from the active GTP-bound form to the inactive GDP-bound form (Li *et al.*, 2005), thereby regulating downstream events leading to changes in the cytoskeleton. It has been shown that Rac1 and Cdc42, downstream of Rho signaling, are regulators of cell spreading and formation of lamellipodia and filopodia (Clark *et al.*, 1998; Hall, 1998), and cell polarization

(Etienne-Manneville and Hall, 2002; Cau and Hall, 2005). Rac1 and Cdc42 regulate laminin-10/11-mediated cell spreading and filopodia formation of the dental epithelium (Fukumoto *et al.*, 2006). Increased expression of RhoGDI in *Amel* $X^{-/-}$/*Ambn*$^{-/-}$ teeth might inhibit active Rho GTP, resulting in irregular ameloblast morphology.

In summary, our study suggests that the enamel matrix proteins such as amelogenins and ameloblastin are not only required for the formation of a proper matrix for well-orchestrated enamel biomineralization, but also have synergistic cellular functions during enamel development.

ACKNOWLEDGMENTS

We thank Drs. Aya Yamada and Yoko Kamasaki for generous help with SEM analysis, and Harry Grant for editorial assistance. This work was supported by the Division of Intramural Research of the National Institute of Dental and Craniofacial Research.

REFERENCES

Bartlett JD, Simmer JP, Xue J, Margolis HC, Moreno EC (1996). Molecular cloning and mRNA tissue distribution of a novel matrix metalloproteinase isolated from porcine enamel organ. *Gene* 183:123-128.

Cau J, Hall A (2005). Cdc42 controls the polarity of the actin and microtubule cytoskeletons through two distinct signal transduction pathways. *J Cell Sci* 118(Pt 12):2579-2587.

Cerný R, Slaby I, Hammarström L, Wurtz T (1996). A novel gene expressed in rat ameloblasts codes for proteins with cell binding domains. *J Bone Miner Res* 11:883-891.

Clark EA, King WG, Brugge JS, Symons M, Hynes RO (1998). Integrin-mediated signals regulated by members of the rho family of GTPases. *J Cell Biol* 142:573-586.

Du C, Falini G, Fermani S, Abbott C, Moradian-Oldak J (2005). Supramolecular assembly of amelogenin nanospheres into birefringent microribbons. *Science* 307:1450-1454; *erratum* in *Science* 309:2166, 2005.

Etienne-Manneville S, Hall A (2002). Rho GTPases in cell biology. *Nature* 420:629-635.

Fong CD, Cerný R, Hammarström L, Slaby I (1998). Sequential expression of an amelin gene in mesenchymal and epithelial cells during odontogenesis in rats. *Eur J Oral Sci* 106(Suppl 1):324-330.

Fukumoto S, Kiba T, Hall B, Iehara N, Nakamura T, Longenecker G, *et al.* (2004). Ameloblastin is a cell adhesion molecule required for maintaining the differentiation state of ameloblasts. *J Cell Biol* 167:973-983.

Fukumoto S, Yamada A, Nonaka K, Yamada Y (2005). Essential roles of ameloblastin in maintaining ameloblast differentiation and enamel formation. *Cells Tissues Organs* 181:189-195.

Fukumoto S, Miner JH, Ida H, Fukumoto E, Yuasa K, Miyazaki H, *et al.* (2006). Laminin alpha5 is required for dental epithelium growth and polarity and the development of tooth bud and shape. *J Biol Chem* 281:5008-5016.

Gibson CW, Yuan ZA, Hall B, Longenecker G, Chen E, Thyagarajan T, *et al.* (2001). Amelogenin-deficient mice display an amelogenesis imperfecta phenotype. *J Biol Chem* 276:31871-31875.

Gibson CW, Kulkarni AB, Wright JT (2005). The use of animal models to explore amelogenin variants in amelogenesis imperfecta. *Cells Tissues Organs* 181:196-201.

Hall A (1998). Rho GTPases and the actin cytoskeleton. *Science* 279: 509-514.

Hall A, Nobes CD (2000). Rho GTPases: molecular switches that control the organization and dynamics of the actin cytoskeleton. *Philos Trans R Soc Lond B Biol Sci* 355:965-970.

Hatakeyama J, Sreenath T, Hatakeyama Y, Thyagarajan T, Shum L, Gibson CW, *et al.* (2003). The receptor activator of nuclear factor-kappa B ligand-mediated osteoclastogenic pathway is elevated in amelogenin-null mice. *J Biol Chem* 278:35743-35748.

Hatakeyama J, Philp D, Hatakeyama Y, Haruyama N, Shum L, Aragon MA, *et al.* (2006). Amelogenin-mediated regulation of osteoclastogenesis and periodontal cell proliferation and igration. *J Dent Res* 85: 144-149.

Hu JCC, Hu Y, Smith CE, McKee MD, Wright JT, Yamakoshi Y, *et al.* (2008). Enamel defects and ameloblast-specific expression in *Enam* knock-out/*lacZ* knock-in mice. *J Biol Chem* 283:10858-10871.

Kim JW, Seymen F, Lin BP, Kiziltan B, Gencay K, Simmer JP, *et al.* (2005). ENAM mutations in autosomal-dominant amelogenesis imperfecta. *J Dent Res* 84:278-282.

Krebsbach PH, Lee SK, Matsuki Y, Kozak CA, Yamada KM, Yamada Y (1996). Full-length sequence, localization, and chromosomal mapping of ameloblastin. A novel tooth-specific gene. *J Biol Chem* 271:4431-4435.

Li Y, Decker S, Yuan ZA, DenBesten PK, Aragon MA, Jordan-Sciutto K, *et al.* (2005). Effects of sodium fluoride on the actin cytoskeleton of murine ameloblasts. *Arch Oral Biol* 50:681-688.

Li Y, Suggs C, Wright JT, Yuan Z, Aragon M, Fong H, *et al.* (2008). Partial rescue of the amelogenin null dental enamel phenotype. *J Biol Chem* 283:15056-15062.

Masuya H, Shimizu K, Sezutsu H, Sakuraba Y, Nagano J, Shimizu A, *et al.* (2005). Enamelin (Enam) is essential for amelogenesis: ENU-induced mouse mutants as models for different clinical subtypes of human amelogenesis imperfecta (AI). *Hum Mol Genet* 14:575-583.

Moradian-Oldak J, Goldberg M (2005). Amelogenin supra-molecular assembly in vitro compared with the architecture of the forming enamel matrix. *Cells Tissues Organs* 181:202-218.

Moradian-Oldak J, Du C, Falini G (2006). On the formation of amelogenin microribbons. *Eur J Oral Sci* 114(Suppl 1):289-296.

Nishikawa S, Kitamura H (1986). Localization of actin during differentiation of the ameloblast, its related epithelial cells and odontoblasts in the rat incisor using NBD-phallacidin. *Differentiation* 30:237-243.

Paine ML, Luo W, Zhu DH, Bringas P Jr, Snead ML (2003a). Functional domains for amelogenin revealed by compound genetic defects. *J Bone Miner Res* 18:466-472.

Paine ML, Wang HJ, Luo W, Krebsbach PH, Snead ML (2003b). A transgenic animal model resembling amelogenesis imperfecta related to ameloblastin overexpression. *J Biol Chem* 278:19447-19452.

Peters MF, Ross CA (2001). Isolation of a 40-kDa Huntingtin-associated protein. *J Biol Chem* 276:3188-3194.

Prakash SK, Gibson CW, Wright JT, Boyd C, Cormier T, Sierra R, *et al.* (2005). Tooth enamel defects in mice with a deletion at the Arhgap 6/ Amel X locus. *Calcif Tissue Int* 77:23-29.

Simmer JP, Fukae M, Tanabe T, Yamakoshi Y, Uchida T, Xue J, *et al.* (1998). Purification, characterization, and cloning of enamel matrix serine proteinase 1. *J Dent Res* 77:377-386.

Takai Y, Sasaki T, Tanaka K, Nakanishi H (1995). Rho as a regulator of the cytoskeleton. *Trends Biochem Sci* 20:227-231.

European Journal of Orthodontics 31 (2009) 536–541
doi:10.1093/ejo/cjp017
Advance Access Publication 15 May 2009

The P561T polymorphism of the growth hormone receptor gene has an inhibitory effect on mandibular growth in young children

Yasunori Sasaki*, Kyoko Satoh*, Haruaki Hayasaki**, Satoshi Fukumoto***, Taku Fujiwara* and Kazuaki Nonaka****

*Department of Pediatric Dentistry, Unit of Translational Medicine, Nagasaki University Graduate School of Biomedical Sciences, Nagasaki, **Department of Pediatric Dentistry, Kagoshima University, Graduate School of Medical and Dental Sciences, ***Department of Oral Health and Development Sciences, Division of Pediatric Dentistry, Tohoku University Graduate School of Dentistry, Sendai and ****Section of Pediatric Dentistry, Division of Oral Health, Growth and Development, Faculty of Dental Science, Kyushu University, Fukuoka, Japan

SUMMARY P561T heterozygous missense mutation in the growth hormone receptor (GHR) is a candidate genetic polymorphism (single-nucleotide polymorphism) for human mandibular growth. The purpose of this study was to assess whether this mutation affects mandibular growth during early childhood. The difference in mandibular growth between P561T heterozygous and wild-type individuals was analysed by cephalometric measurements during childhood. The subjects included 33 children with mandibular protrusion (aged 3–12 years, 16 males and 17 females) and 27 normal children (aged 3–13 years, 14 males and 13 females). Genomic DNA extracted from buccal epithelial cells was genotyped for the P561T heterozygous mutation with a molecular analysis (polymerase chain reaction—restriction fragment length polymorphism method). Two of the patients with normal occlusion and five with mandibular protrusion were heterozygous for the mutation.

Chi-square analysis showed that the frequency of this mutation did not differ statistically between the normal and mandibular protrusion subjects. Multilevel model analysis of the 101 cephalograms showed that the mutation reduced the linear measurements of the mandible. These findings suggest that P561T heterozygous mutation affects mandibular growth during early childhood, and this mutation in the GHR gene is hypothesized to function as an inhibitory factor in the process of mandibular growth.

Introduction

Many factors regulating mandibular growth have been identified in the formation of the mandibular arch (Pirinen, 1995; Mina, 2001). Determining the factors affecting mandibular growth contributes to early diagnosis and treatment of mandibular protrusion. Longitudinal cephalometric observation of the mandibles in offspring produced by a complete Dilallel cross among five strains of rats showed that mandibular size was primarily affected by genetics (Nonaka *et al.*, 1991). Quantitative trait locus (QTL) analysis in an inbred strain of mice was used to determine the chromosomal regions responsible for mandibular length between menton and gonion (Dohmoto *et al.*, 2002). Two significant QTLs were detected within the regions 13cM and 16cM in chromosome 11, including orthodenticle homeobox, suggesting the possibility that some major genes are responsible for mandibular length.

Growth hormone (GH) plays a major role in regulating growth during childhood and adolescence and also regulates metabolism through its binding to the growth hormone transmembrane receptor (GHR; Piwien-Pilipuk *et al.*, 2002). Laron syndrome is caused by the dominant-negative defects of the intracellular domain of GHR, and affected individual have underdevelopment of the facial bones (Laron, 2004). In the Human Gene Mutation Database, 56 different *GHR* gene mutations, including 32 missense and nonsense mutations, have been registered (Stenson *et al.*, 2003). In a few reports concerning the effect of GHR gene mutations on craniofacial growth, Chinese Han individuals with a genomic polymorphism at codon 526 of the GHR gene have a greater mandibular ramus length (Co–Go/Ar–Go) (Zhou *et al.*, 2005). At position 1777 in GHR, a transversion of amino acid from cytosine to adenine changed codon 561 from proline to threonine (P561T), affecting the cytoplasmic domain of the GHR. In the Japanese population, no significant correlation has been observed between body height and P561T variants at the GHR gene locus (Chujo *et al.*, 1996; Yamaguchi *et al.*, 2001), but a relationship has been reported between mandibular ramus length and the heterozygous missense mutation P561T (Yamaguchi *et al.*, 2001). Japanese carrying the P561T variant had a significantly smaller mandibular ramus length (condylion–gonion) than those who were wild type at this locus. These findings suggest that the change in the cytoplasmic domain of GHR produced by P561T does not play a significant role in determining final body height and may affect mandibular growth independently of systemic growth. However, it is currently unclear whether P561T affects craniofacial growth in children.

To determine whether the P561T heterozygous missense mutation affects mandibular growth during the early

stages of growth and development in humans, differences in mandibular growth between wild-type and P561T individuals genotyped with restriction fragment length polymorphism were analysed using cephalometric measurements.

Subjects and methods

All subjects were either patients at the Department of Pediatric Dentistry, Faculty of Dentistry, Kyushu University, or volunteers of their respective families. This study was approved by the ethics committee of Kyushu University Faculty of Dental Science and Nagasaki University, and informed consent was granted by the parents/guardians of all children.

Genetic analysis

Thirty-three Japanese children with mandibular protrusion and 27 'normal' children with a Class I occlusion and without other types of malocclusion, who had no general physical diseases or congenital disorders, participated in this study. As the focus of the research was the effect of a GHR gene polymorphism on mandibular growth, subjects with a Class II occlusion with maxillary protrusion were initially excluded to avoid confusion. Genomic DNA was extracted from buccal epithelial cells and employed as the primary source for polymerase chain reaction (PCR) amplification (Liu *et al.*, 1995; Sasaki *et al.*, 2007). Briefly, buccal epithelia cells were collected by twirling a sterile cytology brush on the inner cheek for 30 seconds. DNA was extracted using a BuccalAmp™ DNA extraction kit (Epicentre, Madison, Wisconsin, USA) according to the manufacturer's protocol. The partial sequence of exon 10 of the GHR gene, which encodes the cytoplasmic domain of GHR, was amplified by PCR using primer pairs deduced from the published DNA sequence (Chujo *et al.*, 1996) and then, the PCR-amplified DNA was digested with *Stu* I, which digests a wild-type GHR gene at codon 561, but not a GHR gene with mutation P561T (Figure 1a,b). DNA samples were analysed by electrophoresis using 1.8 per cent (w/v) agarose gel (Figure 1c). For wild-type subjects, digestion resulted in two restriction fragments of 808 and 229 base pairs (subjects 1, 2, 3, and 7). In contrast, P561T heterozygous subjects showed three bands of 1037, 808, and 229 base pairs (subjects 4, 5, and 6).

Cephalometric analysis

A total of 101 lateral cephalograms were obtained for 24 of the mandibular protrusion subjects and 17 of the normal subjects during the treatment or management period according to the informed consent. Nine of the patients with mandibular protrusion and 10 of the normal subjects were excluded because of the absence of lateral cephalograms.

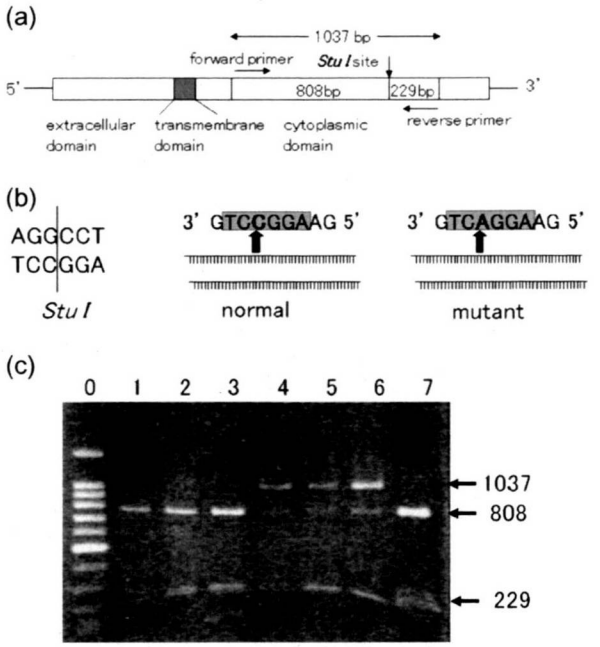

Figure 1 Analysis of the polymerase chain reaction (PCR)–restriction fragment length polymorphism method of the growth hormone receptor (GHR) gene mutation P561T in seven of the 60 subjects was examined. (a) Human GHR cDNA was represented. GHR gene including *Stu* I site (or codon 561) is amplified by PCR using forward and reverse primers. (b) The PCR-amplified DNA was digested by Stu I, which is able to digest the normal GHR gene, but not that with mutation P561T. (c) DNA samples were analysed by electrophoresis using 1.8 per cent (w/v) agarose gel. Lane 0: 100 bp DNA marker.

Of the 101 cephalograms, 43 were from 19 males (mean age: 7 3 ± 2 2 years) and 58 from 22 females (mean age: 7 1 ± 20 1 years). The age range of subjects was from 3 years 3 months to 13 years 3 months. The lateral cephalometric radiographs were analysed according to the landmarks shown in Figure 2. The radiographic enlargement was 100 per cent. Linear measurements associated with mandibular size (Cd–Go, ramus length; Pog'–Go, mandibular body length; and Gn–Cd, mandibular length) and maxillary length (A'–Ptm') and angular measurement associated with Gn–Cd (Ar–Go–Mn) were compared between patients who were either wild type or carried the heterozygous mutation. All the measurements were made with an electric digitizer (model KD 4320, Graphtec Ltd, Yokohama, Japan) online with a computer. The resolution and angular variables were 0.1 mm and 0.2 degrees, respectively.

Statistical analysis

Chi-square analysis was performed to test the difference in mutantion frequencies between the normal and mandibular protrusion subjects. Multilevel model analysis has been previously applied to the analysis of jaw movements (Strenio *et al.*, 1983; Goldstein and Rasbash, 1996) and was used in the present study to evaluate the growth curves. The